

Equation-of-motion treatment of hyperfine interaction in a quantum dot

Changxue Deng and Xuedong Hu

Department of Physics, University at Buffalo, SUNY, Buffalo, NY 14260-1500

Abstract

Isolated electron spins in semiconductor nanostructures are promising qubit candidates for a solid state quantum computer. There have seen truly impressive experimental progresses in the study of single spins in the past two years. In this paper we analytically solve the *Non-Markovian* single electron spin dynamics due to inhomogeneous hyperfine couplings with surrounding nuclei in a quantum dot. We use the equation-of-motion method assisted with a large field expansion in a full quantum mechanical treatment. We recover the exact solution for fully polarized nuclei. By considering virtual nuclear spin flip-flops mediated by the electron, which generate fluctuations in the Overhauser field (the nuclear field) for the electron spin, we find that the decay amplitude of the transverse electron spin correlation function for partially polarized nuclear spin configurations is of the order unity instead of $O(1/N)$ (N being the number of nuclei in the dot) obtained in previous studies. We show that the complete amplitude decay can be understood with the spectrum broadening of the correlation function near the electron spin Rabi frequency induced by nuclear spin flip-flops. Our results show that a 90% nuclear polarization can enhance the electron spin T_2 time by more than one order of magnitude in some parameter regime. In the long time limit, the envelope of the transverse electron spin correlation function has a non-exponential $1/t^2$ decay in the presence of both polarized and unpolarized nuclei.

PACS numbers: 85.35.Be, 76.60.-k, 03.67.Lx,

I. INTRODUCTION

The electron spin dynamics in semiconductor nanostructures is presently of particular interest both experimentally^{1,2,3,4} and theoretically because of the potential applications in spin quantum computation.⁵ Among the many roadblocks to solid state quantum computing, maintaining the quantum coherence of the electron spin in a quantum dot is a crucial issue. One of the most important and relevant spin interactions for this confined electron is hyperfine coupling with the surrounding nuclei, or the so-called Fermi contact interaction. The role of hyperfine interaction could be both negative and positive depending on the actual experimental operations. On the one hand, nuclear spin bath could be a major decoherence channel for the electron spin that acts as a qubit.^{6,7} This problem is unavoidable in a GaAs quantum dot where all the isotopes of Ga and As has nuclear spin $I = \frac{3}{2}$, Although this is not a problem for silicon quantum dot where the nuclei of ^{29}Si ($I = \frac{1}{2}$, with natural abundance 4.68%) could be removed, so that the silicon is made up of only ^{28}Si or ^{30}Si , both having nuclear spin $I = 0$. On the other hand, electron-nuclei hyperfine interaction could also be utilized to control the nuclear spins, which as an ensemble could act coherently. For example it has recently been suggested that the ensemble of nuclear spins in a quantum dot may be used as a long-lived quantum memory for electron spin by transferring the electron spin dynamics to nuclear spin reservoir coherently.⁸

The study of Non-Markovian electron spin dynamics in the presence of hyperfine interaction is a complicated problem due to its quantum many-body (electron and nuclei) nature. The problem has been studied by many researchers previously.^{9,10,11,12,13,14,15} An exact solution⁹ has been found for an electron interacting with the fully polarized nuclear reservoir. Various types of approximations, perturbation theory¹¹ or an effective Hamiltonian approach,^{13,14} have been employed in dealing with this problem. Numerical studies,^{10,12,13} limited by the exponentially large Hilbert space, can only be applied to small systems, typically of up to 20 spins. Here we analyze the problem starting from the exact Hamiltonian using the equation-of-motion (EOM) method by working in the Heisenberg picture. Usually the problem is studied using the master equations for the system density operator.¹⁷ We develop a systematic large field expansion method to simplify the equations dramatically. This way we can address the full quantum mechanical problem analytically using well-controlled approximations.

A confined electron in a gated quantum dot generally has a nonuniform envelope wavefunction and a relatively large radius, which leads to an inhomogeneous hyperfine coupling with the nuclear spins on the crystal lattice. The effective number N of nuclear spins involved is $10^4 - 10^6$ depending on the actual size of the quantum dot. It is exactly this non-uniformity that causes both electron spin relaxation and dephasing. Physically this is because the electron acquires a different phase factor each time it interacts with a particular nuclear spin with random orientation. This effect is totally quantum mechanical, and is quite different from the dephasing effect caused by inhomogeneous broadening or ensemble average (T_2^*) ,¹⁸ which can be removed by spin echo technique.^{2,3}

Electron mediated nuclear spin interactions have been studied for a long time, in both metals and in semiconductors.^{19,20} Although at a finite magnetic field the direct electron-nuclear-spin flip-flop is highly unlikely due to the Zeeman energy mismatch, higher-order processes where electron spin does not flip are possible. For example, conduction-electron-mediated nuclear spin interaction [Ruderman-Kittel-Kasuya-Yoshida (RKKY)] has been studied for a long time in both metals and semiconductors. Here we focus on the electron-mediated RKKY interaction between nuclear spins on *single* mediating electron spin. Specifically we focus on the backaction of this effective nuclear spin interaction on the mediating electron spin and consequent electron spin decoherence. Helped by a systematic large field expansion, we solve the full quantum mechanical problem analytically and reveal the crucial importance of the electron-mediated nuclear spin flip-flop processes in the decoherence of an electron spin.

We note that virtual (high order) processes can be classified into two categories, one involving electron spin flip and the other without electron spin flip. In a high effective field (external plus nuclear field), these two types of processes have completely different consequences. In terms of energy the process with electron spin flip needs large extra energy to compensate the electron Zeeman energy, since the nuclear Zeeman energy is much smaller and can be neglected. Such processes (real processes for the electron), no matter whether they first order or higher orders, are highly unlikely for large fields. Not surprisingly a negligible decay amplitude of order $O(\frac{1}{N})$ for both diagonal (relaxation) and non-diagonal (dephasing) components of the density matrix element of electron spin was found from these processes. In the second category, no extra energy is necessary since there is no electron spin flip between the initial and final states. It is found these kinds of processes indeed

have significant contributions to T_2 using numerical simulation,¹³ though for only 13 nuclear spins from an effective Hamiltonian. To illustrate the role of virtual flip-flopping of nuclear pairs, we shall compare the exact solution of fully polarized nuclei where no virtual nuclear spin-exchange is allowed with that of the case in which one of the nuclear spins is in the down state initially, assuming that all the nuclear spins point up in the fully polarized configuration.

In general, exact solution cannot be found for a non-quadratic Hamiltonian. From the perspective of equations of motion, this means that there is an infinite number of equations when one attempts to evaluate the Green's function. Therefore, a decoupling method has to be applied to cut off the series of equations and close the system. In the usual many-body treatment, this amounts to calculate some *thermal averages* using the spectral functions determined from the Green's functions self-consistently. However, such approximation involving ensemble average is not available in our present case, where we are interested in the *real time* dynamics including the coherent part and the decaying part of a single quantum many-body system. In our study we assume that the effective magnetic field (denoting the total of external and nuclear fields) is large so that the electron Zeeman energy is much larger than the single nuclear spin Zeeman energy, and the direct electron-nuclei flip-flop is not allowed energetically. This assumption greatly simplifies our discussions by selecting one group of equations, which give the major contribution to decoherence. Typically, an effective field slightly larger than the fully polarized nuclear field is enough for obtaining self-consistent result. Our study has experimental relevance since the full Overhauser field is about 4 Tesla in GaAs quantum dots.

The electron spin relaxation induced by spin-orbit interaction is quite slow in QDs because of the level discretization.²¹ Nuclear magnetic dipolar interaction gives rise to spectral diffusion and also leads to dephasing at a time scale of $10 \mu\text{s}$.^{14,22,23} The fluctuation of the nuclear field (the Overhauser field) is due to direct nuclear spin flip-flops. Generally the nuclear dipolar coupling is weaker than the hyperfine interaction in a semiconductor QD. Therefore, it would be interesting to compare the electron spin decoherence times caused by nuclear dipolar coupling and the virtual processes due to hyperfine interaction in the strong field limit.

In this paper we present more detailed and extensive studies than those given in our previous paper.¹⁵ The remainder of the paper is organized as follows: in Section II, we at-

tempt to represent the electron spin decoherence, especially pure dephasing, with a properly constructed Green's function. We set up the equations of motion for calculating the correlation function. In Section III we calculate the Green's functions with several different nuclear polarization for the nuclear spin reservoir. The spectral functions which determine the decay behaviors of the electron spin correlation functions at large time are found. In Section IV and V we discuss the obtained results and conclude the paper.

II. METHOD

The hyperfine interaction between nuclei and electrons in the conduction band of a semiconductor can be modeled by a simple Hamiltonian,^{19,24}

$$H = \omega_0 S^z + \sum_k A_k I_k^z S^z + \sum_k \frac{A_k}{2} (I_k^- S^+ + I_k^+ S^-). \quad (1)$$

Here the first term represents the Zeeman energy of the electron spin with $\omega_0 = g^* \mu_B B_0$; the second and last terms are the hyperfine interaction between the electron spin and the nuclear spins. Between the two, the second term represents the nuclear Overhauser field on the electron, while the last term describes the flip-flop of the electron and nuclear spins. The Zeeman energy of nuclear spins are neglected, because the Hamiltonian in Eq. (1) conserves the total spin angular momentum, and a single spin nuclear Zeeman energy is much less than that of the electron spin. Here A_k is the hyperfine coupling constant at the k th nucleus. It is proportional to the probability of the electron at position \mathbf{r} and may be written as

$$A_k = A |\psi(\mathbf{r}_k)|^2, \quad (2)$$

where $\psi(\mathbf{r})$ is the electron wavefunction (envelope wavefunction and Bloch wavefunction at the site of the nuclear spins). A is the total coupling strength between the electron and the nuclei: $\int A(\mathbf{r}) d\mathbf{r} = A$. In a GaAs quantum dot, $A \approx 90 \mu eV$. It is convenient to work with dimensionless units, and assume $A/N = 1$. This means that energy is measured in units of A/N and time is rescaled by N/A , with $\hbar = 1$. A general form of A_k will make the summation over k quite complicated when looking for analytical results, especially for anisotropic three-dimensional quantum dots. A simple form, which is appropriate for two-dimensional gated quantum dots and has been used in previous calculations,¹¹

$$A_k = e^{-\frac{k}{N}}, \quad (3)$$

is adopted in the following calculations. Here N is the effective number of nuclear spins in the dot. This coupling describes a two dimensional quantum dot with electron wavefunction decreases as a Gaussian as the distance from the center of the quantum dot increases. The index k labels the radial coordinate r^2 . $A = \int_0^\infty A_k dk = N$. In other words, A and N can be used interchangeably.

The central quantity that we are going to calculate is the retarded Green's function of the localized spin state

$$G_\perp(t) = -i\theta(t)\langle\Psi_0|S^-(t)S^+(0)|\Psi_0\rangle. \quad (4)$$

Here $\theta(t)$ is the step function. Ψ_0 is the initial wavefunction of the system (including electron and nuclear spins),

$$|\Psi_0\rangle = [\alpha_0|\downarrow\rangle + \beta_0|\uparrow\rangle]|\psi_n\rangle. \quad (5)$$

We assume that the electron and nuclear spins are in a product state at $t = 0$, and are therefore not entangled. Furthermore, we assume that initially nuclear spins are in a product state $|\psi_n\rangle = |I_1^z, I_2^z, \dots, I_k^z, \dots\rangle$, where $I_k^z = \uparrow$ or \downarrow , i.e., nuclear spins could be either up or down at some particular site with a total net nuclear spin polarization P that will be defined later. Here we assume that the magnitude of nuclear spin is $1/2$ although $I=3/2$ for all the isotopes of GaAs. This assumption simplifies the algebras in the following study though we do not anticipate this simplification to cause any qualitative difference in the properties of $G_\perp(t)$. A mixed nuclear spin state could be expressed in terms of a linear combination of the product states. Thus, the results of our calculations of product states can be used to study more general initial nuclear states directly.

An important quantity that represents the quantum coherence of the electron spin is the quantum mechanical expectation values of transverse electron spin operators, $\langle\Psi_0|S^-(t)|\Psi_0\rangle$ or similarly $\langle\Psi_0|S^+(t)|\Psi_0\rangle$. The Green's function defined in Eq. (4) is equivalent to $\langle\Psi_0|S^-(t)|\Psi_0\rangle$ in the high field limit. Substituting Eq. (5) into the expression $\langle\Psi_0|S^-(t)|\Psi_0\rangle$, we find

$$\langle\Psi_0|S^-(t)|\Psi_0\rangle = \alpha_0^*\beta_0\langle\downarrow, \psi_n|e^{iHt}S^-e^{-iHt}|\uparrow, \psi_n\rangle + \text{higher order terms}. \quad (6)$$

Among higher order contributions, one or more electron spin flips can lead to non-zero results. However, as we have argued in the introduction that these terms are of the order

$O(1/N)$ or $O(1/N^n)$ for polarized nuclei in the absence of external an external magnetic field. The leading order contribution in Eq.(6) on the contrary does not involve any electron spin flip during the evolution. In fact this term gives rise to pure dephasing (as the electron spin does not flip) while the higher order terms involving electron spin flip lead to decoherence induced by relaxation. The leading order term in Eq. (6) is exactly the Green's function defined in Eq.(4) up to a proportional constant with the assumption that $|\Psi_0\rangle = |\downarrow, \psi_n\rangle$. Another way to understand the pure dephasing term in Eq. (6) is to consider the phase evolution of the electron spin in the Schödinger picture,

$$\begin{aligned} G_{\perp}(t) &= -i\theta(t)\langle\downarrow; I_{k_1}^z, \dots, I_{k_N}^z | e^{iHt/\hbar} S^- e^{-itH/\hbar} S^+ | \downarrow; I_{k_1}^z, \dots, I_{k_N}^z \rangle \\ &= -i\theta(t) \left\{ \langle\downarrow; I_{k_1}^z, \dots, I_{k_N}^z | e^{iHt/\hbar} \right\} S^- \left\{ e^{iHt/\hbar} | \uparrow; I_{k_1}^z, \dots, I_{k_N}^z \rangle \right\}. \end{aligned} \quad (7)$$

The term in the first curly brackets represents the evolution of the electron spin-down state in the presence of the hyperfine interaction, while the term in the second curly brackets represents the evolution of the electron spin-up state in the same environment. If no electron spin flip occurs, any decay in the calculated average will be due solely to dephasing between the electron spin-up and spin-down states. Obviously, electron spin flip will also cause decay of the correlation function. Therefore, $G_{\perp}(t)$ contains the complete decoherence information for the electron spin in consideration.

Without loss of generality, we assume $|\Psi_0\rangle = |\downarrow, \psi_n\rangle$ in the following discussions. The equation of motion can be set up in the Heisenberg representation

$$i\frac{d}{dt}G_{\perp}(t) = \delta(t) - i\theta(t)\langle\Psi_0|[S^-(t), H]; S^+(0)|\Psi_0\rangle. \quad (8)$$

The solution of this equation can be obtained in the energy space by performing the Fourier transformation, after which we have an equation in the form of the standard equation of motion for the correlation function of two arbitrary operators

$$\omega\langle\langle\hat{A}; \hat{B}\rangle\rangle_{\omega} = \langle\Psi_0|\hat{A}\hat{B}|\Psi_0\rangle_{t=0} + \langle\langle[\hat{A}, H]; \hat{B}\rangle\rangle_{\omega}, \quad (9)$$

where expectation value in the first term on the right hand side is calculated at the initial time, and $\langle\langle\hat{A}; \hat{B}\rangle\rangle_{\omega} \equiv \int (-i)\theta(t)\langle\Psi_0|\hat{A}(t)\hat{B}(0)|\Psi_0\rangle e^{i\omega t} dt$.

Although the hyperfine Hamiltonian [Eq. (1)] looks quite simple, the general solution has not been found. Instead one could obtain approximate solutions under various conditions.

Exact solutions can be found in two simple cases: namely the system with fully polarized initial nuclear spin configuration, and the Hamiltonian with uniform coupling constants.

It is straightforward to derive the following equations of $G_{\perp}(\omega)$ by calculating the spin commutators repeatedly,

$$\begin{aligned}
(\omega - \Omega_0)G_{\perp}(\omega) &= 1 - \sum_k A_k \langle \langle n_k S^-; S^+ \rangle \rangle_{\omega} - \sum_k A_k \langle \langle I_k^- S^z; S^+ \rangle \rangle_{\omega}, \\
(\omega^2 - \frac{A_k^2}{4}) \langle \langle I_k^-; S^+ \rangle \rangle_{\omega} &= -\frac{A_k}{2} (\omega + \frac{A_k}{2}) G_{\perp}(\omega) + \omega A_k \langle \langle n_k S^-; S^+ \rangle \rangle_{\omega} + \frac{1}{2} \sum_{k'(k)} A_k A_{k'} V_{kk'}(\omega), \\
(\omega^2 - \frac{A_k^2}{4}) \langle \langle I_k^- S^z; S^+ \rangle \rangle_{\omega} &= \frac{A_k^2}{4} \langle \langle n_k S^-; S^+ \rangle \rangle_{\omega} - \frac{A_k}{4} (\omega + \frac{A_k}{2}) G_{\perp}(\omega) + \omega \sum_{k'(k)} \frac{A_{k'}}{2} V_{kk'}(\omega), \quad (10)
\end{aligned}$$

with

$$V_{kk'}(\omega) = \langle \langle I_k^- S^+ I_{k'}^-; S^+ \rangle \rangle_{\omega} - \langle \langle I_k^- I_{k'}^+ S^-; S^+ \rangle \rangle_{\omega}, \quad (11)$$

where $n_k = \frac{1}{2} - I_k^z$ and $\Omega_0 = \omega_0 + \frac{N}{2}$. Here Ω_0 is the effective magnetic field for fully polarized nuclear spin reservoir. $\sum_{k'(k)}$ represents the summation over k' for $k' \neq k$. After rearranging the equations, we find

$$\begin{aligned}
[\omega - \Omega_0 - \Sigma_0(\omega)] G_{\perp}(\omega) &= 1 - \sum_k A_k \langle \langle n_k S^-; S^+ \rangle \rangle_{\omega} - \frac{\omega}{2} \sum_{k \neq k'} \frac{A_k A_{k'}}{(\omega^2 - A_k^2/4)} V_{kk'}(\omega) \quad (12) \\
&\quad - \frac{1}{4} \sum_k \frac{A_k^3}{(\omega^2 - A_k^2/4)} \langle \langle n_k S^-; S^+ \rangle \rangle_{\omega}
\end{aligned}$$

with the self-energy

$$\Sigma_0(\omega) = \frac{1}{4} \sum_k \frac{A_k^2}{\omega - A_k/2}. \quad (13)$$

We will use $\Omega = \omega_0 + \sum_k A_k I_k^z$ to represent the effective magnetic field experienced by the electron in the following discussion. The meanings of the various correlations are obvious. For example, $\langle \langle n_k S^-; S^+ \rangle \rangle_{\omega}$ represents the Fourier transform of the time-correlation function for flipping the electron spin to the down state while the k th nuclear spin is also in the down state ($n_k = 1$). Both $\langle \langle I_k^-; S^+ \rangle \rangle_{\omega}$ and $\langle \langle I_k^- S^z; S^+ \rangle \rangle_{\omega}$ describe the direct electron-nuclear-spin flip-flop. The only difference is that the latter one depends on the electron spin state. $1/\Omega$ will be taken as an important expansion parameter in next section where we look for solutions

of the Eqs. (10). $\Omega \sim N$ corresponds to polarized nuclei or external magnetic field with a few Tesla's. $\Omega \gg 1$ will be a good starting point for simplifying the EOMs. $\langle\langle n_k S^-; S^+ \rangle\rangle_\omega$ and $V_{kk'}(\omega)$ are higher order correlation functions. We should mention that the Eqs. (10) are exact. Approximations will be applied to obtain the general solution of arbitrary nuclear polarization when $\Omega \sim N$. We will repeatedly use two different approximations, large N expansion and large field expansion. These two terms have different meanings. The first one is just a mathematical treatment, where we simply neglect A_k when A_k and Ω appear together since $A_k \sim 1$. This approximation simplifies our EOMs significantly. The large field expansion, which will only be used for solving the high frequency solution of the partially polarized and unpolarized nuclei, is a physical approximation, where we select a group of EOMs that describe the major contributions to the self-energies.

III. SOLUTIONS OF THE GREEN'S FUNCTION

In this section we obtain the solutions $G_\perp(\omega)$ of Eq. (10) presented in Section II under various conditions. The real time dynamics of the Green's function, $G_\perp(t)$ can be found using the spectral function $\rho(\omega)$,

$$G_\perp(t) = -i\theta(t) \int_{-\infty}^{\infty} \rho(\omega) e^{-i\omega t} d\omega, \quad (14)$$

where the spectral function $\rho(\omega)$ is obtained by analytical continuation ($\omega \rightarrow \omega + i0^+$) using the retarded Green's function $G_\perp(\omega)$ ²⁵

$$\rho(\omega) = -\frac{1}{\pi} \text{Im} G_\perp(\omega + i0^+). \quad (15)$$

The imaginary part of the retarded Green's function contains contributions from poles and branch cuts.²⁵ More specifically, the poles will determine the renormalized energy or the oscillation frequencies of the electron spin in our case; while the branch cut describes the decay of the electron spin state. Our focus in this section is to calculate these quantities for various nuclear spin polarization, with or without external magnetic field.

A. Fully polarized nuclei reservoir

The solution to the problem of an electron spin interacting with a fully polarized nuclear spin reservoir is quite straightforward. One crucial argument we will use to simplify the

EOMs is the conservation of angular momentum at any time during the evolution. For initially fully polarized nuclei (all nuclear spins in the up state) and initial wave function $\Psi_0 = |\downarrow, \psi_n\rangle$, this means that there is only one spin (either the electron spin or one of the nuclear spins) in the down state. This restriction eliminates all the higher-order correlation functions present in Eq. (12). For example, $\langle\langle n_k S^-; S^+ \rangle\rangle_\omega = 0$ because when the electron spin is flipped down, $n_k = 1/2 - I_k^z$ must be zero for fully polarized nuclei. $V_{kk'}(\omega)$ vanishes for the same reason. Therefore Eq. (12) can be reduced to

$$G_\perp(\omega) = \frac{1}{\omega - \Omega_0 - \Sigma_0(\omega)}, \quad (16)$$

where $\Omega_0 = \omega_0 + N/2$ for fully polarized nuclei. Assuming that the hyperfine coupling constant takes the form in Eq. (3), the real and imaginary part of the self-energy are

$$\text{Re}\Sigma_0(\omega) = \frac{1}{4} \int_0^\infty \frac{A_k^2}{\omega - \frac{A_k}{2}} dk = -\frac{N}{2} - N\omega \ln \left| 1 - \frac{1}{2\omega} \right|, \quad (17)$$

and

$$\text{Im}\Sigma_0(\omega) = -\frac{\pi}{4} \int_0^\infty A_k^2 \delta\left(\omega - \frac{A_k}{2}\right) dk = -N\pi\omega, \text{ for } 0 < \omega < \frac{1}{2}. \quad (18)$$

In both calculations we convert the summation over k into an integration, and use the formula

$$\sum_k \delta\left(\omega \pm \frac{A_k}{2}\right) = \mp \frac{N}{\omega}, \quad (19)$$

in finding the imaginary part. The imaginary part of the self energy is nonzero only when $\frac{1}{2} > \omega > 0$, this is due to the constraint of the delta function in Eq. (18). The spectral function can be calculated with Eq. (15)

$$\rho(\omega) = \begin{cases} Z_p \delta(\omega - \Omega - \text{Re}\Sigma_0) & \omega \sim N \\ -\frac{1}{N\omega} \frac{1}{\left[\frac{\omega_0}{N\omega} + \frac{1}{N} + \ln\left|1 - \frac{1}{2\omega}\right|\right]^2 + \pi^2} & 0 < \omega < \frac{1}{2}, \end{cases} \quad (20)$$

where the renormalization factor Z_p is²⁵

$$Z_p = \frac{1}{\left|1 - \frac{\partial \Sigma_0(\omega)}{\partial \omega}\right|_{\omega_p}}. \quad (21)$$

The pole ω_p is the solution of equation $\omega - \Omega - \text{Re}\Sigma_0(\omega) = 0$. When $\omega_0 = 0$ (zero external field), $\omega_p \approx N/2 + 1/4$ and $Z_p \approx 1 - 1/N$. It is clear from Eq. (20) that there are two

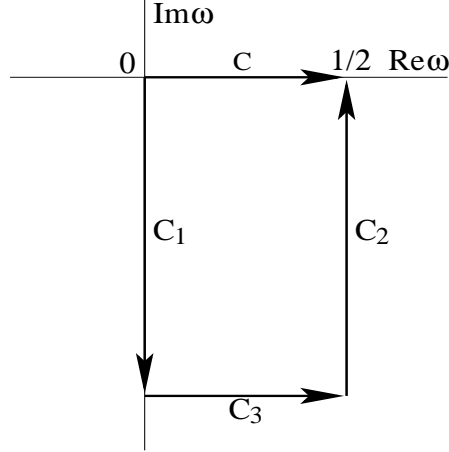


FIG. 1: To obtain the asymptotic behavior of $G_{\perp}(t)$ at large time, the Fourier integral in Eq. (14) is converted into a Laplace integral by deforming the original contour C into $C_1 + C_2 + C_3$ as shown above and then allowing $\omega \rightarrow \infty$.

contributions to the spectral function $\rho(\omega)$, namely a pole near Ω and a branch cut in the range of $[0, \frac{1}{2}]$. For a schematic, see left panel of Fig. (2). In the fully polarized case, the weight of the pole is of order $O(1)$, while only a small fraction of the spectral function is a continuous spectrum. Since only the branch cuts or continuous spectrum contribute to the decoherence, electron spin in a fully polarized nuclear environment has an infinite T_2 time.

In Appendix A we show that this exact solution can also be found with the Jordan-Wigner representation by reducing the original spin Hamiltonian into the non-interacting Anderson impurity model.²⁶ The physical meaning from the exact solution of the Anderson model is that part of the time the electron spin (localized state) is in the spin-down state, and part of the time one of nuclear spins (continuous state) occupies the down state. The true eigenstates (resonant scattering) are the linear combinations of these two states.

In order to obtain real time dynamics we need to perform an inverse Fourier transform. This is straightforward for the delta function part of $\rho(\omega)$, the contribution of the pole. However the branch cut integration is much more complicated, and a closed form cannot be found. To investigate the long time decay of the Green's function, the method of the steepest descent²⁷ is used. The approximate calculation of the integration is justified by carefully deforming the integration contour in the complex ω plane so that Laplace's method can be used. In Laplace's method the integration of an exponential function is approximated by

the integral of this function in the neighborhood of the global maximum of the integrand. In order to use the method of steepest descent to calculate the frequency integral in Eq. (14), we deform the original integration contour C into C_1 , C_2 , and C_3 as shown in Fig. 1. The integration along C_3 at infinity in the lower half plane is exponentially small in the large time limit. This is exactly the spirit of steepest descent, as one can see the term $e^{-i\omega t}$ is negligible if ω is analytically extended to the complex plane through $\omega = -is$ and s is allowed to approach positive infinity. Substituting the spectral function into Eq. (14) we obtain

$$G_{\perp}(t) = \left[1 + \mathcal{O}\left(\frac{1}{N}\right)\right] e^{i\frac{N}{2}t} - \frac{1}{N} \int_0^{\frac{1}{2}} \frac{1}{\omega} \frac{e^{-i\omega t} d\omega}{\left[\frac{1}{N} + \ln\left|1 - \frac{1}{2\omega}\right|\right]^2 + \pi^2}, \quad (22)$$

where we have neglected the factor $-i\theta(t)$ in Eq. (14) and assumed that $\omega_0 = 0$. On the contour C_1 where $\omega = -is$, the integral is determined by the integration interval near $s = 0^+$ as $t \rightarrow +\infty$ because of the term e^{-st} . By performing a Taylor expansion around $s = 0^+$ we obtain $\rho_{\perp}(-is) = -\frac{i}{s \ln s}$. The asymptotic form of the integral for the inverse Fourier transform when $t \rightarrow \infty$ is

$$G_{\perp}(t) = \left[1 + \mathcal{O}\left(\frac{1}{N}\right)\right] e^{i\frac{N}{2}t} + \frac{1}{N} \left[\frac{1}{\ln t} + \left(\ln 2 - \ln \gamma + i\frac{\pi}{2}\right) \frac{1}{(\ln t)^2} \right] + \mathcal{O}\left[\frac{1}{N} \frac{1}{(\ln t)^3}\right], \quad (23)$$

where $\gamma = -\int_0^{\infty} \ln s e^{-s} ds$ is the Euler constant. It can be shown that the integral along C_3 has a smaller contribution that is proportional to $\frac{1}{N t \ln t}$. The amplitude of the decay part is only of the order $\mathcal{O}\left(\frac{1}{N}\right)$, and the leading order behavior at long time is $1/\ln t$. We have written the oscillatory part as $[1 + \mathcal{O}\left(\frac{1}{N}\right)]e^{i\frac{N}{2}t}$, where we have neglected the $1/N$ correction of the coefficient. The results thus agree with those found previously.⁹

B. One-spin-flipped nuclear reservoir

The exact solution for the fully polarized nuclear reservoir is instructive but of little practical relevance in current experimental situations, where maximum achievable nuclear polarization in semiconductor quantum dots is in the order of 50%. A pertinent question is whether there is any qualitative difference between partially polarized and non-polarized nuclear reservoirs in the spectral function, spin correlation, and its decoherence. To address

this question, we consider another simple case in which there is only one flipped nuclear spin in the otherwise fully polarized initial state, i.e., $|\Psi_0\rangle = |\downarrow; \uparrow_1, \uparrow_2, \dots, \downarrow_{\bar{k}}, \dots, \uparrow_N\rangle$, where \bar{k} is the index of the initially flipped nuclear spin.

The EOMs are quite complicated even for this simple case. In Appendix B we give the complete EOMs, including all the higher-order correlation functions. Together with Eq. (12), these six equations form a closed set. The even higher-order correlation functions vanish because of conservation of angular momentum, as we have discussed in the case of the fully polarized nuclear reservoir. We point out that these equations are exact. They are obtained from the iterative EOMs by calculating the commutators. It is a formidable task to find the exact solution of these equations, thus we first simplify the equations as much as we can. It turns out to be convenient to discuss the low energy ($|\omega| < \frac{1}{2}$) and high energy ($\omega \sim \Omega$) solutions separately. From the exact solution of the fully polarized case, we already know that the spectral function behaves quite differently in these two regimes. Specifically, the low energy part corresponds to a continuous spectrum, while the high energy part is just a delta function that gives rise to the undamped coherent oscillation in the electron spin. In the following we shall discuss both the low energy and high energy solutions of one-flipped nuclear spin reservoir with $1/N$ expansion. Since N is very large, this approximation should make little difference from the exact solutions.

Low energy solution. To obtain the low energy solution, we start from Eq. (12). By examining the right hand side of Eq. (12), it is easy to see that one needs to find $\langle\langle n_k S^-; S^+ \rangle\rangle_\omega$ and $V_{kk'}(\omega)$ [Recall that $V_{kk'}(\omega) = \langle\langle I_k^- S^+ I_{k'}^-; S^+ \rangle\rangle_\omega - \langle\langle I_k^- I_{k'}^+ S^-; S^+ \rangle\rangle_\omega$]. To simplify the equations, we use the fact that $\omega \ll \Omega$ in the low energy regime and $A_k \ll \Omega$. As we point out in the introduction, we assume the existence of a large effective field so that $\Omega \sim N$. Therefore we can use the approximation, $\omega \pm \Omega \mp \frac{A_k + A_{k'}}{2} \approx \pm \Omega$. In other words, we can neglect ω and A_k whenever they appear in a sum with Ω . This approximation helps find the leading order solutions. From Eq. (B1), we obtain $\langle\langle n_k S^-; S^+ \rangle\rangle_\omega$,

$$\langle\langle n_k S^-; S^+ \rangle\rangle_\omega = -\frac{1}{\Omega + \Sigma_0(\omega)} \langle n_k \rangle_0 + \frac{\omega}{2[\Omega + \Sigma_0(\omega)]} \sum_{k'(k)} \frac{A_k A_{k'}}{\omega^2 - \frac{A_k^2}{4}} V_{kk'}(\omega) + \mathcal{O}\left(\frac{1}{\Omega^2}\right). \quad (24)$$

Here the self-energy term $\Sigma_0(\omega)$ is of the order $\mathcal{O}(N)$ because it involves a summation over nuclear sites [also see Eqs. (18) for the fully polarized nuclear reservoir]. By studying Eq. (10) and the equations in Appendix B one can draw the conclusion that $V_{kk'}(\omega) \sim \langle\langle n_k S^-; S^+ \rangle\rangle_\omega$. This is because $V_{kk'}(\omega) \sim \langle\langle I_k^- S^-; S^+ \rangle\rangle_\omega / \Omega$, which is a result

of Eq. (B4). By putting this relation into Eq. (10) one could immediately see that $V_{kk'}(\omega) \sim \langle\langle n_k S^-; S^+ \rangle\rangle_\omega$. With these results we can determine the order of magnitude of the summation $\sum_k A_k \langle\langle n_k S^-; S^+ \rangle\rangle_\omega$ using Eq. (24)

$$\sum_k A_k \langle\langle n_k S^-; S^+ \rangle\rangle_\omega \propto \frac{1}{\Omega + \Sigma_0(\omega)} \sum_k \langle n_k \rangle_0 \propto O\left(\frac{1}{\Omega}\right), \quad (25)$$

since $\sum_k \langle n_k \rangle_0 = 1$. [Recall that there is only one nuclear spin in the down state ($n_{\bar{k}} = 1$) initially, and all other nuclear spins point up ($n_k = 0$)]. Similarly one can easily find that both the third and the fourth terms on the right hand side of Eq. (12) are of the order $O\left(\frac{1}{\Omega}\right)$. Therefore we obtain the leading order low energy solution of $G_\perp(\omega)$ from Eq. (12)

$$G_\perp(\omega) = -\frac{1}{\Omega + \Sigma_0(\omega)} + O\left(\frac{1}{\Omega^2}\right), \quad (26)$$

for $\omega \sim O(1)$. This solution is exactly the leading order approximation of the fully polarized nuclei in the low energy limit. Clearly there are only higher-order differences for the two cases in this regime. The leading order spectral functions also have the same behavior.

High energy solution. The approximate solution in the high energy limit is much more difficult to obtain compared to the low energy limit. In this limit $\omega \sim \Omega$, thus $A_k \ll \omega, \Omega$. Generally we can drop A_k in the expressions such as $\omega \pm \frac{A_k}{2}$ and $\Omega \pm \frac{A_k}{2}$. However, we must be careful when dealing with terms like $\omega - \Omega \pm \frac{A_k}{2}$. Since both ω and Ω are of order N , the difference between them could be $O(1)$. Thus we can no longer neglect the A_k terms in these expressions. With $\Omega \gg A_k$, we find Eq. (B2) can be simplified to

$$\langle\langle n_k S^-; S^+ \rangle\rangle_\omega = \frac{1}{\omega - \Omega - \Sigma_0(\omega)} \left[\langle n_k \rangle_0 - \frac{1}{4\Omega} (f_k + g_k) \right], \quad (27)$$

where $f_k(\omega) = \sum_{k''} A_{k''} V_{k''k}(\omega)$ and $g_k(\omega) = \sum_{k''} A_{k''} V_{kk''}(\omega)$. Substituting Eq. (27) into Eq. (12), we obtain

$$G_\perp(\omega) = \frac{1}{\omega - \Omega - \Sigma_0(\omega)} \left[1 - \frac{1}{2\Omega} \sum_{k \neq k'} A_k A_{k'} V_{kk'}(\omega) \right]. \quad (28)$$

Here $V_{kk'}(\omega)$ contains two terms, one of which is negligible compared to the other in the high energy limit. It can be shown that $\langle\langle I_k^- S^+ I_{k'}^-; S^+ \rangle\rangle_\omega \sim O\left(\frac{1}{\Omega}\right) \langle\langle I_k^- I_{k'}^+ S^-; S^+ \rangle\rangle_\omega$. This relationship is to be expected as $\langle\langle I_k^- S^+ I_{k'}^-; S^+ \rangle\rangle_\omega$ corresponds to the electron being flipped during the evolution, which is a probability event $\left[O\left(\frac{1}{N}\right)\right]$. Similar simplifications will be sought when we search for solutions of partially polarized and unpolarized nuclei.

In order to evaluate $V_{kk'}(\omega)$, we first simplify Eqs. (B3) and (B5) using the large N expansion method we have outlined above. It can be shown that the two equations can be approximated with

$$\langle\langle I_k^- n_{k'}; S^+ \rangle\rangle_\omega = -\frac{A_k}{2\Omega} \langle\langle n_{k'} S^-; S^+ \rangle\rangle_\omega + \frac{A_{k'}}{2\Omega} V_{kk'}(\omega), \quad (29)$$

and

$$\langle\langle I_k^- I_{k'}^+ I_{k''}^-; S^+ \rangle\rangle_\omega = \frac{A_k}{2\Omega} V_{k''k'}(\omega) + \frac{A_{k''}}{2\Omega} V_{kk'}(\omega). \quad (30)$$

Using Eqs. (B4), (29), and (30), we can derive an implicit equation for $V_{kk'}(\omega)$,

$$\begin{aligned} \left(\tilde{\omega} + \frac{A_k + A_{k'}}{2} \right) V_{kk'}(\omega) &= -\frac{A_k A_{k'}}{4\Omega} \frac{\langle n_k \rangle_0}{\omega - \Omega - \Sigma_0 + A_k} - \frac{A_k A_{k'}}{4\Omega} \frac{\langle n_{k'} \rangle_0}{\omega - \Omega - \Sigma_0 + A_{k'}} \\ &+ \frac{1}{4\Omega} [A_k g_{k'}(\omega) + A_{k'} f_k(\omega)], \end{aligned} \quad (31)$$

where $\tilde{\omega} = \omega - \Omega - \frac{A_2}{4\Omega}$ and $A_2 = \sum_k A_k^2$. Using the wavefunction in Eq. (2), it is easy to show that $A_2 = \frac{N}{2}$. Multiplying both sides of Eq. (31) by $A_{k'}/[\tilde{\omega} + (A_k + A_{k'})/2]$ and summing over k' , we find the equation for $f_k(\omega)$ takes the form

$$\begin{aligned} (\Omega - \alpha_k) f_k &= -\frac{\alpha_k A_k \langle n_k \rangle_0}{\omega - \Omega - \Sigma_0 + A_k} - \frac{A_k A_k^2}{4 \left(\tilde{\omega} + \frac{A_k + A_k}{2} \right) (\omega - \Omega - \Sigma_0 + A_k)} \\ &+ \frac{1}{4} \sum_{k''(k)} \frac{A_k A_{k''}}{\left(\tilde{\omega} + \frac{A_k + A_{k''}}{2} \right)} g_{k''}, \end{aligned} \quad (32)$$

where

$$\alpha_k(\tilde{\omega}) = \frac{1}{4} \sum_{k''} \frac{A_{k''}^2}{\tilde{\omega} + \frac{A_k + A_{k''}}{2}}. \quad (33)$$

The equation for g_k is obtained by interchanging f_k and g_k in Eq. (32). Through the symmetry of the equations for f_k and g_k , we find $f_k = g_k$ in the leading order large Ω expansion. From Eq. (32) it can be seen that $\sum_k A_k f_k \sim \mathcal{O}(1)$ near the pole of $1/(\omega - \Omega - \Sigma_0)$.

Equation (32) can be transformed to an integral equation by converting the summations into integrals, though this integral equation is still difficult to solve. For our present purpose, Eq. (28) and Eq. (32) are enough to further our discussions. First, by solving the equation $\omega - \Omega - \Sigma_0(\omega) = 0$, we obtain the same pole as the fully polarized case. The interesting point here is that the pole now has a reduced weight, because the residue is $Z_p \approx 1 - \frac{1}{N} - \frac{1}{2\Omega} \sum_k A_k f_k$. Since $\sum_k A_k f_k \sim \mathcal{O}(1)$ when $\omega - \Omega - \Sigma_0 = 0$, the difference from the

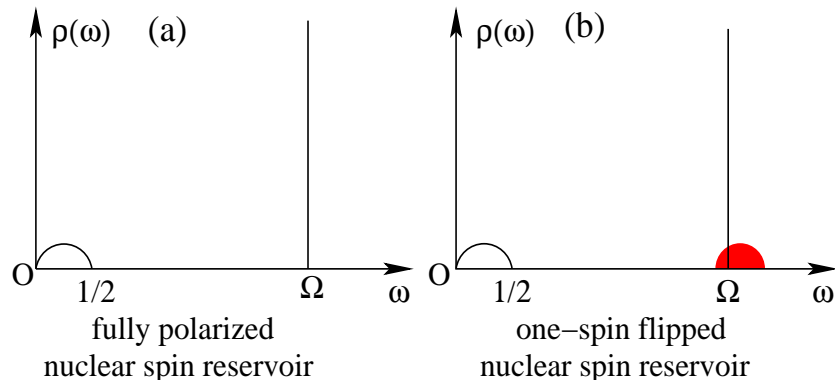


FIG. 2: Schematic of the spectral function for fully polarized nuclei (left panel) and one-spin flipped nuclei (right panel). The shaded area in the right figure denotes the contribution of the branch cut by considering virtual nuclear spin flip-flop which is not possible in the case of fully polarized nuclei. Also the delta function represented by the vertical line has a slightly reduced weight compared to that in the fully polarized case.

fully polarized nuclei is very small ($Z_p \approx 1 - 1/N$ in the exact solution). On the other hand, the function $f_k(\omega)$ has non-vanishing imaginary part when the frequency is in the neighborhood of Ω . In other words, the spectral function has a branch cut near Ω . This contribution to the spectral function is only of the order $O\left(\frac{1}{\Omega}\right)$ because of the prefactor $\frac{1}{2\Omega}$ in Eq. (28). Combining these discussions with the picture we have established in the low frequency region, we can summarize the properties of the spectral function in the right panel of Fig. 2. In the left panel, we draw the schematic of the spectral function of the exact solution in the fully polarized case for comparison. It is quite easy to understand where the new feature comes from. In the fully polarized case, the only possible process is the electron-nuclei flip-flop (see the upper figure in Fig. 3). The electron flipped state is a high energy state, where energy $\hbar\Omega$ (neglecting the nuclear Zeeman energy) is needed to compensate for the Zeeman energy mismatch. For a one-spin-flipped nuclei reservoir, virtual nuclear spin flip-flop mediated by the electron is possible (see the lower figure in Fig. 3). In the initial and final states, the electron spin state remains unchanged, but two nuclear spins exchange their states. The virtual (intermediate) state is a high energy state, and the cross section of this process is proportional to $1/\Omega$.

C. Partially polarized and unpolarized nuclear reservoir

The solutions of both the fully polarized nuclear reservoir and one spin flipped nuclear reservoir, while instructive, have little experimental relevance. It is important to find the solution for a general nuclear spin configuration when studying the electron spin decoherence. To proceed, we first define the effective nuclear polarization P by

$$P = \frac{N_{\uparrow} - N_{\downarrow}}{N}, \quad (34)$$

where N_{\uparrow} (N_{\downarrow}) represents the number of nuclear spins with up (down) spin. We further assume that both N_{\uparrow} and N_{\downarrow} are large, i.e., $N_{\uparrow} \sim N_{\downarrow}$. We can then convert the summation over both the up and down nuclear spins into integrals. We expect the solution to be similar to those we have already found in the limit of highly polarized nuclei when $N_{\downarrow} \ll N_{\uparrow}$ or $N_{\downarrow} \gg N_{\uparrow}$.

We treat the nuclear field (or Overhauser field) $\sum_k A_k I_k^z$ with the adiabatic approximation. With a large effective magnetic field Ω , the electron spin precesses with frequency $\frac{\Omega}{\hbar}$. On the other hand, the nuclear field fluctuates around its average value by a small amount in a much slower time scale, since there are many nuclear spins ($N \gg 1$) interacting with the electron spin simultaneously. Each of the nuclear spins has only a $1/N$ probability to exchange spin with the electron. Under this approximation we can neglect the small time-dependent change of the nuclear field $\sum_k A_k I_k^z$, and factor it out from the time-dependent correlation function $\langle\langle \sum_k A_k I_k^z(t) S^-(t); S^+ \rangle\rangle$. Meanwhile, the nuclear spin raising and lowering operators are treated fully quantum mechanically. This approximation reduces the higher order correlation function $\langle\langle n_k S^-; S^+ \rangle\rangle_{\omega}$ to $G_{\perp}(\omega)$. The term $\sum_k A_k I_k^z S^z$ in the Hamiltonian remains as an operator for calculating commutators. When we take the nuclear operator in the correlation functions as a c-number, we always make sure that the difference from the real quantity only gives rise to higher order contributions.

Similar to the highly polarized situations discussed previously, we study the solution in the low energy and high energy limit separately. Recall that in the case of polarized nuclear reservoir with one flipped spin, the weight of the delta function in the spectral function is reduced by a small amount, and there appears a new continuous contribution to the spectral function near Ω because of the nuclear spin flip-flop mediated by the electron. Since there is only one nuclear spin in the down state initially, scattering channels for nuclear flip-flops are limited (see Fig. 3). Therefore, decoherence effect of the continuous contribution is small,

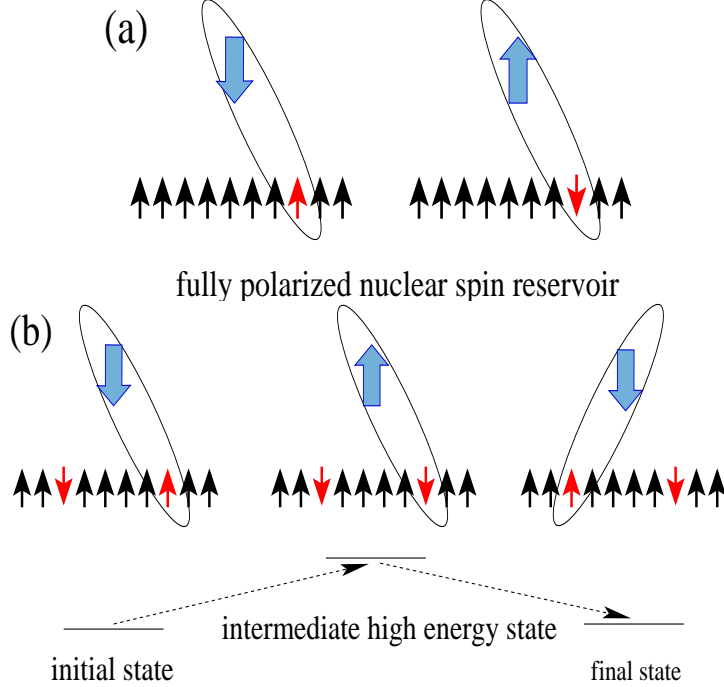


FIG. 3: Schematic of possible spin exchange processes in case of fully polarized nuclei (upper panel) and one-spin-flipped nuclei (lower panel). For the fully polarized nuclei, the only possible process is the direct electron-nuclei flip-flop, which requires a large assisted energy to compensate in a high magnetic field. Second-order virtual processes are also accessible for the one-spin-flipped nuclei. In this case, the high energy state is an intermediate state, while the electron spin state is not changed in the initial and final states, and two nuclear spins exchange information effectively.

of order $O\left(\frac{1}{N}\right)$. With more nuclei in the down spin state, we expect that the continuous contribution will become increasingly important, and be of the order unity eventually when $N_{\downarrow} \sim N_{\uparrow}$. We will verify this conjecture in the following discussions.

Low energy solution. Helped by the adiabatic approximation for the nuclear field, we can write the first equation in Eqs. (10) in the following form,

$$G_{\perp}(\omega) = -\frac{1}{\Omega} + \frac{1}{\Omega} \sum_k A_k \langle\langle I_k^- S^z; S^+ \rangle\rangle_{\omega} + O\left(\frac{1}{\Omega^2}\right). \quad (35)$$

Thus the leading order contribution to $G_{\perp}(\omega)$ is $O\left(\frac{1}{\Omega}\right)$. We can also write the equations for $\langle\langle I_k^-; S^+ \rangle\rangle_{\omega}$ and $\langle\langle I_k^- S^z; S^+ \rangle\rangle_{\omega}$ as

$$\omega \langle\langle I_k^-; S^+ \rangle\rangle_{\omega} = A_k \langle\langle I_k^- S^z; S^+ \rangle\rangle_{\omega} - h_k G_{\perp}(\omega), \quad (36)$$

$$\omega \langle\langle I_k^- S^z; S^+ \rangle\rangle_{\omega} = -\frac{h_k}{2} G_{\perp}(\omega) + \frac{A_k}{4} \langle\langle I_k^-; S^+ \rangle\rangle_{\omega} + \frac{1}{2} \langle\langle I_k^- V; S^+ \rangle\rangle_{\omega}, \quad (37)$$

with $h_k = A_k \langle I_k^z \rangle_0$ and $V = S^+ \sum_k A_k I_k^- - \sum_k A_k I_k^+ S^-$. By introducing h_k , we are taking a mean field average for the Overhauser field produced by this individual nucleus. Substituting Eqs. (36) and (37) into Eq. (35), we obtain

$$\left(\omega^2 - \frac{A_k^2}{4} \right) \langle \langle I_k^- S^z; S^+ \rangle \rangle_\omega = -\frac{h_k}{2} \left(\omega + \frac{A_k}{2} \right) G_\perp(\omega) + \frac{\omega}{2} \langle \langle I_k^- V; S^+ \rangle \rangle_\omega. \quad (38)$$

Fortuitously, further calculation of $\langle \langle I_k^- V; S^+ \rangle \rangle_\omega$ does not lead to any other higher order correlation functions in the low ω limit. This is illustrated by evaluating both $\langle \langle I_k^- S^+ \tilde{I}^-; S^+ \rangle \rangle_\omega$ and $\langle \langle I_k^- \tilde{I}^+ S^-; S^+ \rangle \rangle_\omega$ with the EOM by a $1/N$ expansion. Here we have defined $\tilde{I}_n^\pm = \sum_k A_k^n I_k^\pm$ as collective nuclear spin operators. The index is dropped when $n = 1$. Neglecting all higher order terms, we find

$$\begin{aligned} \Omega \langle \langle I_k^- S^+ \tilde{I}^-; S^+ \rangle \rangle_\omega &= -h_k \langle \langle I_k^- \left(\frac{1}{2} - S^z \right); S^+ \rangle \rangle_\omega \\ &- \langle \tilde{I}_2^z \rangle_0 \langle \langle I_k^- \left(\frac{1}{2} - S^z \right); S^+ \rangle \rangle_\omega + \langle \langle I_k^- \tilde{I}^+ \tilde{I}^-; S^+ \rangle \rangle_\omega, \\ \Omega \langle \langle I_k^- \tilde{I}^+ S^-; S^+ \rangle \rangle_\omega &= -\langle I_k^- \tilde{I}^+ \left(\frac{1}{2} - S^z \right) \rangle_0 \\ &- \langle \tilde{I}_2^z \rangle_0 \langle \langle I_k^- \left(\frac{1}{2} - S^z \right); S^+ \rangle \rangle_\omega + \langle \langle I_k^- \tilde{I}^+ \tilde{I}^-; S^+ \rangle \rangle_\omega, \end{aligned} \quad (39)$$

where we have used the operator equality $S^+ S^- = \frac{1}{2} - S^z$ and the fact that $\langle \langle I_k^- S^+ \tilde{I}^-; S^+ \rangle \rangle_\omega \sim \mathcal{O} \left[\langle \langle I_k^- S^+ \tilde{I}_2^-; S^+ \rangle \rangle_\omega \right]$. Combining Eq. (36) with (39), we find a single equation for $\langle \langle I_k^- S^z; S^+ \rangle \rangle_\omega$ and $G_\perp(\omega)$,

$$\begin{aligned} \left(\omega^2 - \frac{A_k^2}{4} \right) \langle \langle I_k^- S^z; S^+ \rangle \rangle_\omega &= \frac{\omega A_k}{4\Omega} - \frac{P A_k^2}{8} G_\perp(\omega) + \frac{P^2 N A_k}{32\Omega} G_\perp(\omega) \\ &+ \frac{P A_k}{8\Omega} \sum_{k'} A_{k'}^2 \langle \langle I_{k'}^- S^z; S^+ \rangle \rangle_\omega. \end{aligned} \quad (40)$$

In this equation, we have used the mean field average and, replaced the nuclear spin expectation value of the z component $\langle I_k^z \rangle_0$ by the average nuclear polarization $\frac{P}{2}$. The summation $\sum_k A_k^2 \langle \langle I_k^- S^z; S^+ \rangle \rangle_\omega$ in Eq. (40) can be found by multiplying both sides of the equation by $\frac{A_k^2}{\omega^2 - A_k^2/4}$ and then performing the summation over k . We then obtain

$$\sum_k A_k^2 \langle \langle I_k^- S^z; S^+ \rangle \rangle_\omega = \frac{8\omega\sigma_3 + (P^2 N \sigma_3 - 4P\Omega\sigma_4)G_\perp}{32\Omega + 4P\sigma_3}, \quad (41)$$

with

$$\sigma_n(\omega) = \sum_k \frac{A_k^n}{\omega^2 - \frac{A_k^2}{4}}. \quad (42)$$

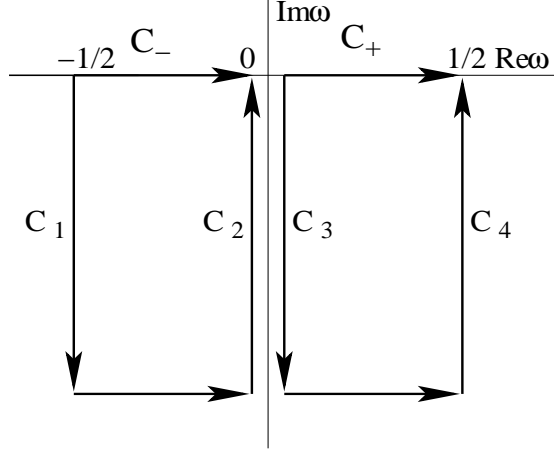


FIG. 4: To obtain the asymptotic behavior of $G_{\perp}(t)$ for partially polarized nuclei at long time limit, the Fourier integral in Eq. (14) is converted into a Laplace integral by deforming the original contour C_+ and C_- into C_1 , C_2 , C_3 , and C_4 as shown above and then allowing $\omega \rightarrow \infty$.

$\sigma_n \sim N$ since it is a summation over all the nuclear spins. Plugging Eq. (41) back into Eq. (40), we obtain an expression for $\sum_k A_k \langle \langle I_k^- S^z; S^+ \rangle \rangle_{\omega}$, which can then be used to find $G_{\perp}(\omega)$ using Eq. (35). After all these evaluations, we obtain the low energy solution for $G_{\perp}(\omega)$:

$$G_{\perp}(\omega) = -8 \frac{8\Omega - 2\omega\sigma_2 + P\sigma_3}{(8\Omega + P\sigma_3)^2 - P^2\sigma_2(2N + \sigma_4)}. \quad (43)$$

The final solution is quite complicated. One important result is that $G_{\perp}(\omega) \sim O(\frac{1}{N})$, just like in the highly polarized cases. In this solution the higher-order correlation function has no effect since the term $\langle \langle I_k^- \tilde{I}^+ \tilde{I}^-; S^+ \rangle \rangle_{\omega}$, which involves nuclear spin flip-flop, does not appear in Eq. (40). The summation $\sigma_n(\omega)$ can be calculated with the same technique as we have used for calculating $\Sigma_0(\omega)$ with analytical continuation ($\omega \rightarrow \omega + i0^+$) and the conversion of summation to integral ($\sum_k \rightarrow \int_0^{\infty} dk$). The real and imaginary parts of σ_n are evaluated and given in Appendix C. The real parts of σ_n have two branch cuts, one from 0 to $\frac{1}{2}$; the other one from $-\frac{1}{2}$ to 0. The imaginary part of $G_{\perp}(\omega)$ is non-zero only in these regions.

We first consider the case of zero external magnetic field, when $\Omega = \frac{PN}{2}$. To study the long time behavior we again deform the original integration contours C_+ and C_- into C_1 , C_2 , C_3 , and C_4 in Fig. 4. The integrals at minus infinity in the lower half plane are neglected. Using the results of $\sigma_n(\omega)$ given in the Appendix C, we find the spectral function behaves

as

$$\rho(0^\mp - is) = \frac{i(P \pm 1)}{2NP} \frac{1}{s \ln s}, \quad (44)$$

on contour C_2 ($\omega = 0^- - is$) and C_3 ($\omega = 0^+ - is$) as s approaches 0^+ . Calculating the Laplace transform, we then obtain the long time asymptotic form of time dynamics of the Green's function in the low energy limit,

$$G_\perp(t) \propto \frac{1}{PN} \frac{1}{\ln t}, \quad t \rightarrow \infty. \quad (45)$$

The long time asymptotic form $1/\ln t$ is the same as that of the fully polarized case, and we do have the right numerical limit as $P \rightarrow 1$. Consider now the situation of the strong Zeeman field limit where $|\omega_0| \gg N$. The Green's function is proportional to $\frac{1}{\Omega}$ when $\omega \ll N$. The asymptotic behavior of $G_\perp(t)$ will be $\frac{1}{t}$, and the decaying amplitude is proportional to $\frac{1}{\Omega}$. Again this result is the same as the fully polarized nuclei case.^{9,11}

The properties of the low energy solution to the spin correlation function studied in this subsection are quite similar to those that have been investigated in previous studies.^{9,11} The basic result is that the decay amplitude is of the order $O\left(\frac{1}{N}\right)$ in the perturbative limit when the effective magnetic field is comparable to the number of nuclear spins in the QD. However, only the direct electron-nuclei flip-flop has been considered in these studies. Therefore it is quite reasonable that the contribution is small since the Zeeman energy mismatch is large.

High energy solution. In the following discussion we search for the solution to the spin correlation function in the high frequency region. This solution will be of the most experimental relevance. In the case of a highly polarized nuclear reservoir the major contribution to the spectral function in the large ω limit is a delta function, that does not lead to any decoherence in the electron spin. When the effect of the electron mediated nuclear spin exchange is included, decoherence with a small amplitude arises. The question is whether this effect will become large enough so that there is a measurable contribution to electron spin dephasing when initially the two nuclear spin species (up and down) have approximately equal population. We address this question in the following discussion of the high energy solution for partially polarized and unpolarized nuclei.

By using the adiabatic approximation and considering that $\omega = \Omega + O(1)$ and $\omega \gg A_k$, Eq. (12) can be straightforwardly simplified to

$$\left(\omega - \Omega - \frac{A_2}{4\Omega}\right) G_\perp(\omega) = 1 - \frac{1}{2\Omega} \sum_{k \neq k'} A_k A_{k'} \langle\langle I_k^- I_{k'}^+ S^-; S^+ \rangle\rangle_\omega, \quad (46)$$

where $A_2 = \sum_k A_k^2$. Notice that $\langle\langle I_k^- S^+ I_{k'}^-; S^+ \rangle\rangle_\omega \ll \langle\langle I_k^- I_{k'}^+ S^-; S^+ \rangle\rangle_\omega$, because $\langle\langle I_k^- I_{k'}^+ S^-; S^+ \rangle\rangle_\omega$ is proportional to $\frac{1}{\omega - \Omega + (A_k - A_{k'})/2}$, while $\langle\langle I_k^- S^+ I_{k'}^-; S^+ \rangle\rangle_\omega$ is proportional to $\frac{1}{\omega + \Omega}$. Mathematically, the difference originates from the commutators of S^\pm with S^z , i.e., $[S^\pm, S^z] = \mp S^\pm$. Since $\omega = \Omega + O(1)$, it is clear that $\frac{1}{\omega - \Omega + (A_k - A_{k'})/2} \sim O(1)$ while $\frac{1}{\omega + \Omega} \sim O(\frac{1}{2\Omega})$. Physically this difference is also easy to understand. In $\langle\langle I_k^- S^+ I_{k'}^-; S^+ \rangle\rangle_\omega$ an electron spin needs to be flipped down, while in $\langle\langle I_k^- I_{k'}^+ S^-; S^+ \rangle\rangle_\omega$, the electron spin is flipped up and then flipped down, and two nuclear spins at k and k' flip-flop with each other. Therefore the process in $\langle\langle I_k^- I_{k'}^+ S^-; S^+ \rangle\rangle_\omega$ does not require a real electron spin flip and is a nuclear flip-flop process mediated by the electron. From Eq. (46) it is clear that this is the only higher-order correlation function that contribute to $G_\perp(\omega)$.

The calculation of the one-pair correlation function $\langle\langle I_k^- I_{k'}^+ S^-; S^+ \rangle\rangle_\omega$ is non-trivial, since its computation involves two-pair correlation function $\langle\langle I_{k_1}^- I_{k_2}^+ I_{k_3}^- I_{k_4}^+ S^-; S^+ \rangle\rangle_\omega$, which in turn depends on even higher order correlation functions. We thus need a cut-off scheme to close the EOM. This is not a problem for the low energy solution where the terms of the one-pair correlation functions cancel each other so that the transverse electron spin Green's function only depends on the electron-nuclei spin-flip correlation functions $\langle\langle I_k^-; S^+ \rangle\rangle_\omega$ and $\langle\langle I_k^- S^z; S^+ \rangle\rangle_\omega$. In the high energy regime, it turns out that the self-energy function can be expanded in powers of $\frac{N}{4\Omega}$. Therefore, as long as the effective field Ω is sufficiently large compared to N (meaning that the applied field is larger than the Overhauser field from a fully polarized nuclear spin reservoir), the approximate solution can be obtained with the first few terms in the expansion.

We start with the exact EOM for $\langle\langle I_k^- I_{k'}^+ S^-; S^+ \rangle\rangle_\omega$,

$$\begin{aligned} & \left(\omega - \Omega + \frac{A_k - A_{k'}}{2} \right) \langle\langle I_k^- I_{k'}^+ S^-; S^+ \rangle\rangle_\omega = h_{k'} \langle\langle I_k^- \left(\frac{1}{2} + S^z \right); S^+ \rangle\rangle_\omega \\ & - A_{k'} \left(\frac{1}{2} + I_{k'}^z \right) \langle\langle I_k^- S^z; S^+ \rangle\rangle_\omega - \langle\langle I_k^- I_{k'}^+ \sum_{k''(k,k')} A_{k''} I_{k''}^- S^z; S^+ \rangle\rangle_\omega. \end{aligned} \quad (47)$$

The leading order (in terms of $\frac{1}{\Omega}$) EOM for $\langle\langle I_k^- I_{k'}^+ \sum_{k''(k,k')} A_{k''} I_{k''}^- S^z; S^+ \rangle\rangle_\omega$ takes the form

$$\begin{aligned} & \omega \langle\langle I_k^- I_{k'}^+ \sum_{k''(k,k')} A_{k''} I_{k''}^- S^z; S^+ \rangle\rangle_\omega = -\frac{A_2}{4} \langle\langle I_k^- I_{k'}^+ S^-; S^+ \rangle\rangle_\omega \\ & - \frac{A_k}{4} \langle\langle I_{k'}^+ \sum_{k''(k,k')} I_{k''}^- S^-; S^+ \rangle\rangle_\omega, \end{aligned} \quad (48)$$

where two-pair correlation functions have been neglected. In leading order of $1/\Omega$, the EOMs of the two lowest-order correlation functions of electron-nuclei flip-flopping in Eq. (10) are

simplified to

$$\langle\langle I_k^-; S^+ \rangle\rangle_\omega = -\frac{P}{2\Omega} A_k G_\perp(\omega), \quad (49)$$

and

$$\langle\langle I_k^- S^z; S^+ \rangle\rangle_\omega = -\frac{A_k}{4\Omega} G_\perp - \frac{1}{2\Omega} \langle\langle I_k^- \sum_{k'(k)} I_{k'}^+ S^-; S^+ \rangle\rangle_\omega, \quad (50)$$

Combining Eq. (47) with Eq. (50) we find the following equation for $\langle\langle I_k^- I_{k'}^+ S^-; S^+ \rangle\rangle_\omega$,

$$\begin{aligned} & \left(\tilde{\omega} + \frac{A_k - A_{k'}}{2} \right) \langle\langle I_k^- I_{k'}^+ S^-; S^+ \rangle\rangle_\omega = \frac{1 - P^2}{8\Omega} A_k A_{k'} G_\perp(\omega) \\ & + \frac{A_{k'}}{4\Omega} \langle\langle I_k^- \sum_{k''(k,k')} A_{k''} I_{k''}^+ S^-; S^+ \rangle\rangle_\omega + \frac{A_k}{4\Omega} \langle\langle I_{k'}^+ \sum_{k''(k,k')} A_{k''} I_{k''}^- S^-; S^+ \rangle\rangle_\omega. \end{aligned} \quad (51)$$

with $\tilde{\omega} = \omega - \Omega - \frac{A_2}{4\Omega}$, which represents the deviation of the frequency from Ω in the high energy limit. Note that $A_2/\Omega \sim O(1)$. Equation (51) is hard to solve because of the summation on the right hand side of the equation. We thus look for an approximate solution in the leading order of $\frac{N}{\Omega}$ in the large Ω limit ($\Omega \gg N$). It is clear by examining the equation that the last two terms on the right hand side of the equation makes a higher order contribution, and can be neglected in a large field expansion. Dividing both sides of Eq. (51) by $\tilde{\omega} - \frac{A_k - A_{k'}}{2}$ and performing the summation over k' , we obtain

$$\langle\langle I_k^- \tilde{I}^+ S^-; S^+ \rangle\rangle_\omega = \left[\frac{1 - P^2}{8\Omega} A_k \sum_{k'} \frac{A_{k'}^2}{\tilde{\omega} + \frac{A_k - A_{k'}}{2}} + O\left(\frac{N^2}{16\Omega^2}\right) \right] G_\perp(\omega). \quad (52)$$

One can solve for $\langle\langle \tilde{I}^- I_{k'}^+ S^-; S^+ \rangle\rangle_\omega$ following a similar approach,

$$\langle\langle \tilde{I}^- I_{k'}^+ S^-; S^+ \rangle\rangle_\omega = \left[\frac{1 - P^2}{8\Omega} A_{k'} \sum_k \frac{A_k^2}{\tilde{\omega} + \frac{A_k - A_{k'}}{2}} + O\left(\frac{N^2}{16\Omega^2}\right) \right] G_\perp(\omega). \quad (53)$$

We then substitute Eqs. (52) and (53) into Eq. (51) to obtain the solution for $\langle\langle I_k^- I_{k'}^+ S^-; S^+ \rangle\rangle_\omega$. Finally we use Eq. (46) to find the Green's function in the high energy limit. The result is

$$G_\perp(\omega) = \frac{1}{\tilde{\omega} - \frac{1 - P^2}{16\Omega^2} \Sigma_1(\tilde{\omega}) - \frac{1 - P^2}{64\Omega^3} [\Sigma_2(\tilde{\omega}) + \Sigma_3(\tilde{\omega})]} \quad (54)$$

where

$$\Sigma_1(\tilde{\omega}) = \sum_{k,k'} \frac{A_k^2 A_{k'}^2}{\tilde{\omega} + \frac{A_k - A_{k'}}{2}}, \quad (55)$$

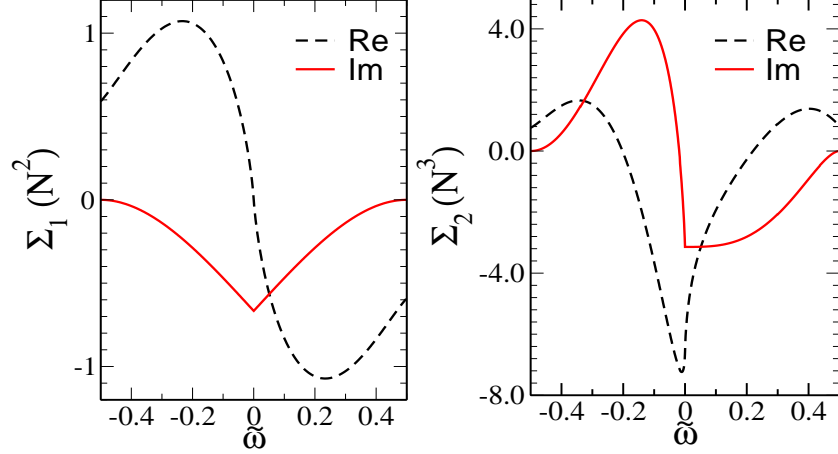


FIG. 5: The self-energies $\Sigma_1(\tilde{\omega})$ (left panel) and $\Sigma_2(\tilde{\omega})$ (right panel) as functions of $\tilde{\omega} = \omega - \Omega - A_2/\Omega$. In these numerical calculations, we have assumed that the hyperfine coupling constant takes the form as in Eq. (2). Both the real part (dashed line) and imaginary part (solid line) of the self-energies are plotted.

$$\Sigma_2(\tilde{\omega}) = \sum_{k,k',k''} \frac{A_k^2 A_{k'}^2 A_{k''}^2}{(\tilde{\omega} + \frac{A_k - A_{k'}}{2})(\tilde{\omega} + \frac{A_{k''} - A_{k'}}{2})}, \quad (56)$$

and

$$\Sigma_3(\tilde{\omega}) = \sum_{k,k',k''} \frac{A_k^2 A_{k'}^2 A_{k''}^2}{(\tilde{\omega} + \frac{A_k - A_{k'}}{2})(\tilde{\omega} + \frac{A_{k''} - A_{k'}}{2})}. \quad (57)$$

Because $\Sigma_1(\tilde{\omega})$ has two summations over nuclear spins, $\Sigma_1(\tilde{\omega}) \sim N^2$. For the same reason, $\Sigma_2(\tilde{\omega})$ and $\Sigma_3(\tilde{\omega})$ are proportional to N^3 . In the above derivation, we have neglected the difference between $\sum_{k''(k,k')}$ and $\sum_{k''}$, which only gives an order unity contribution to the three self-energies. The final expression of $G_{\perp}(\omega)$ we have found in Eq. (54) is of order $O(1)$, in contrast to the solution in the low-energy limit.

The evaluation of self-energies $\Sigma_1(\tilde{\omega})$, $\Sigma_2(\tilde{\omega})$, and $\Sigma_3(\tilde{\omega})$ is quite complicated. In Appendix D we first show that $\Sigma_2(\tilde{\omega}) = \Sigma_3(\tilde{\omega})$. After converting the summations into integrals, we then perform two-dimensional and three-dimensional integrations for $\Sigma_1(\tilde{\omega})$ and $\Sigma_2(\tilde{\omega})$. In Fig. 5, we plot the real and imaginary parts for both of the self-energy terms as a function of the shifted frequency $\tilde{\omega}$. We can see that there is a cusp at $\tilde{\omega} = 0$ for the imaginary parts of both $\Sigma_1(\tilde{\omega})$ and $\Sigma_2(\tilde{\omega})$. Let us first take a closer look at $\Sigma_1(\tilde{\omega})$. Notice that $\text{Im}\Sigma_1(\tilde{\omega})$ is negative for the whole region of $\tilde{\omega}$. This ensures that the spectral function $\rho(\tilde{\omega})$ is always

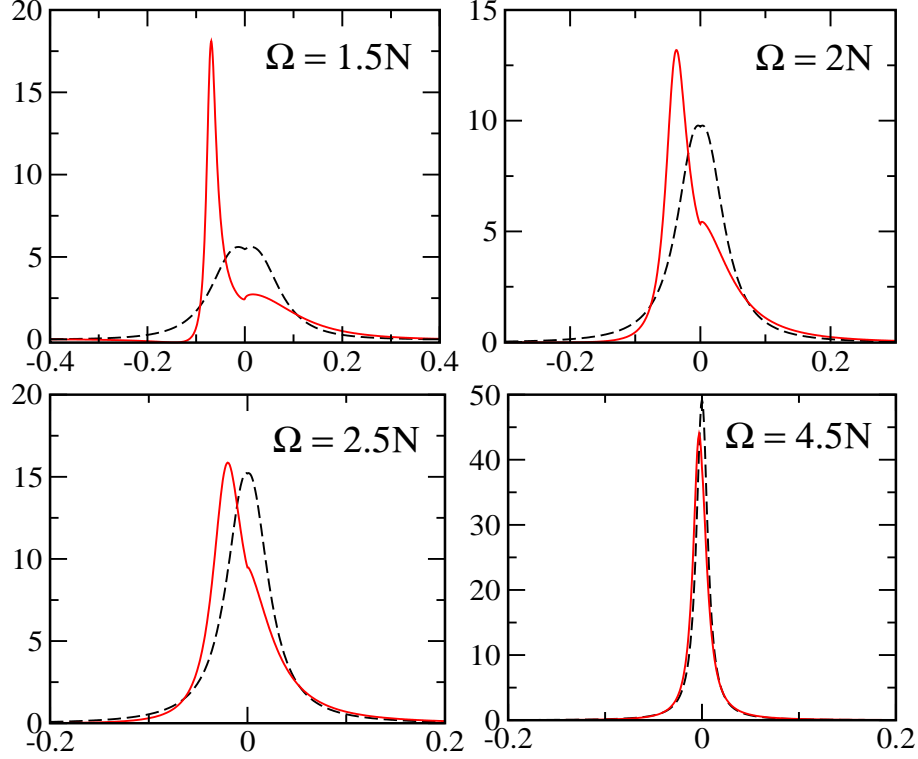


FIG. 6: The spectral function $\rho(\tilde{\omega})$ in the high energy limit as a function of the shifted frequency $\tilde{\omega}$. We have plotted the spectral function for $\Omega = 1.5N$, $\Omega = 2N$, $\Omega = 2.5N$, and $\Omega = 4.5N$. In each of these cases, we have calculated $\rho(\tilde{\omega})$ with two approximations. In the first one, we have evaluated $\rho(\tilde{\omega})$ with only $\Sigma_1(\tilde{\omega})$ (dashed line); and in the other one, we have used both $\Sigma_1(\tilde{\omega})$ and $\Sigma_2(\tilde{\omega})$ (solid line). The lower figures clearly show the success of our large field expansion method. These plots also illustrated the idea that the original delta function in the spectral function is broadened to a continuous spectral function after the virtual nuclear spin flip-flop is included in the calculations.

positive. Like $\text{Im}\sigma_n(\omega)$ [see Eq. (42) and Appendix C], which is nonzero when $-\frac{1}{2} < \omega < \frac{1}{2}$, $\text{Im}\Sigma_1(\tilde{\omega})$ does not vanish when $-\frac{1}{2} < \tilde{\omega} < \frac{1}{2}$. The behavior of $\Sigma_2(\tilde{\omega})$ is very different from $\Sigma_1(\tilde{\omega})$. Neither the real nor the imaginary part of $\Sigma_2(\tilde{\omega})$ is symmetrical about $\tilde{\omega} = 0$. On the other hand, $\text{Im}\Sigma_2(\tilde{\omega})$ changes sign near $\tilde{\omega} = 0$. This leads to no contradiction because $\Sigma_2(\tilde{\omega})$ is a higher order correction term to $\Sigma_1(\tilde{\omega})$, and $\Sigma_2(\tilde{\omega})$ by itself has no physical meaning. Fig. 5 shows that the absolute values of $\Sigma_2(\tilde{\omega})$ are generally larger than those of $\Sigma_1(\tilde{\omega})$, these self-energy terms are multiplied by $\frac{N^2}{16\Omega^2}$ and $\frac{N^3}{64\Omega^3}$, respectively, in Eq. (54), so that $\Sigma_1(\tilde{\omega})$ is still the leading order contribution.

So far the two-pair correlation function has been neglected when deriving the EOMs. If we keep the two-pair correlation function and all the other corresponding functions of the same order, but neglect the three-pair correlation functions, we would find two more higher-order self-energy terms which are proportional to $\frac{N^4}{(4\Omega)^4}$ and $\frac{N^5}{(4\Omega)^5}$. In principle, we can perform the large field expansion to higher and higher orders, and eventually, we should arrive at a finite geometrical series of $\frac{N}{4\Omega}$. We would get a finite instead of an infinite series because there is a finite number (N) of nuclear spins in the quantum dot, and there can be at most N_\downarrow (N_\uparrow) pairs of flip-flopping nuclear spins if $N_\downarrow < N_\uparrow$ ($N_\uparrow < N_\downarrow$). This gives rise to a natural cut-off of self-energy terms in our large field expansion. However, even extension of the calculation to the order of $\frac{N^4}{(4\Omega)^4}$ and $\frac{N^5}{(4\Omega)^5}$ is already very complicated. Nevertheless, the approximation with the first two self-energy terms should be accurate enough as long as the total effective magnetic field Ω is large compared with N (representing the Overhauser field produced by a polarized nuclei spin reservoir).

The validity of our large field expansion method is illustrated in Fig. 6, where we have computed and plotted the spectral function $\rho(\tilde{\omega})$ for various Ω . To compare, we have calculated $\rho(\tilde{\omega})$ using only the self-energy $\Sigma_1(\tilde{\omega})$ and both $\Sigma_1(\tilde{\omega})$ and $\Sigma_2(\tilde{\omega})$. In the two upper panel figures, where Ω is not very large, the contribution of $\Sigma_2(\tilde{\omega})$ is comparable to $\Sigma_1(\tilde{\omega})$. In this case, one needs to calculate more higher order terms of self-energy in the expansion to achieve convergence. When $\Omega = 2.5N$, the difference is already not so significant; and when $\Omega = 4.5N$, we can clearly see that the contribution of $\Sigma_2(\tilde{\omega})$ is negligible. Therefore, our results should be accurate enough as long as $\Omega > 2.5N$. For unpolarized nuclei, $\Omega = 2.5N$ corresponds roughly to an external field of 5 Tesla's for GaAs dots.²⁸

We have checked the sum rule for the spectral function, $\int_{-\infty}^{\infty} \rho(\tilde{\omega}) d\tilde{\omega} = 1$, in all the numerical calculations. We find that the sum rule is always satisfied within 10^{-3} . Fig. 6 also shows that the original delta function $\delta[\omega - \Omega + O(1)]$ without decoherence has been broadened to a continuous spectrum after the electron-mediated flip-flop of nuclear spins are explicitly considered. The sum rule from the continuous spectrum clearly indicates that there is no contribution from a delta-function to the spectral function, so that the decay of $G_\perp(t)$ should be complete.

Once the spectral function is obtained, the electron spin dephasing time T_2 can be estimated as the half-width of the spectrum at $\tilde{\omega} = 0$ peak, i.e., $T_2 = 1/\Delta\tilde{\omega}$. The result is shown in Fig. 7, where the dephasing time is plotted as functions of the nuclear polarization

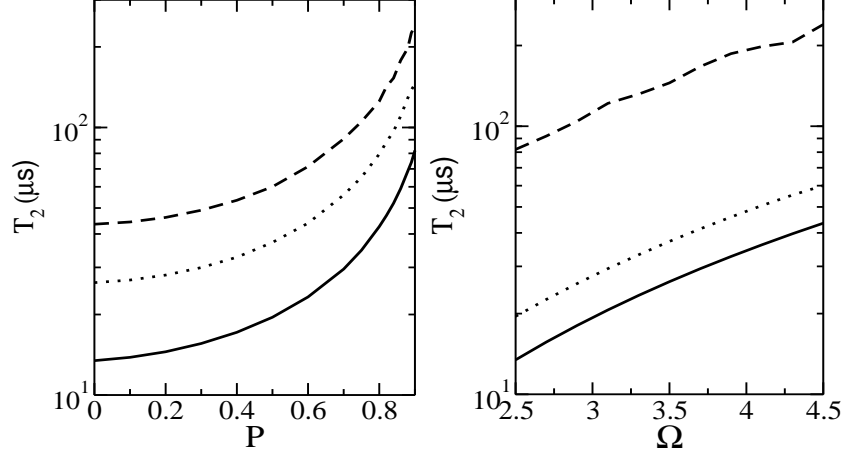


FIG. 7: The electron spin T_2 time in logarithm scale as a function of nuclear spin polarization P (left panel) and the effective magnetic field Ω (right panel). T_2 is estimated with the spectral function by finding the half-width of the spectral peak. It is easy to see that the coherence time can greatly enhanced by increasing the nuclear polarization to 80%. We have assumed $A = 92 \mu\text{eV}$ in these calculations.

P and the effective magnetic field Ω . In all the numerical calculations, we have assumed the summed hyperfine coupling constant $A = \sum_k A_k = 92 \mu\text{eV}$. Fig. 7 indicates that to increase T_2 , polarizing the nuclear spins is more effective than increasing the external magnetic field. In essence, increasing P leads to a reduction to in the phase space for nuclear spin flip-flop, while increasing Ω leads to increased energy for the intermediate state and thus reduced cross-section for the higher-order process. The T_2 time can be enhanced by almost one order of magnitude by increasing P from 0 to 90%, while applying higher magnetic fields extends the coherence time by a few times. For unpolarized nuclei with $\Omega = 2.5N$, we find $T_2 \approx 10$ microsecond, which is similar to the decoherence time caused by the nuclear dipole-dipole interaction. This comparison needs to be kept in perspective, however, since our numerical results are calculated for an effectively two-dimensional QD with Gaussian type wave function, while the previous results for dipolar coupling are obtained for a 3-dimensional QD.²² It would be interesting to explore how dimensionality changes the T_2 times quantitatively. In addition, our results are obtained by assuming nuclear spin $I = \frac{1}{2}$ throughout this paper, though all the isotopes of Ga and As nuclei have spin $I = \frac{3}{2}$. Exploration of the dimension and I dependence of T_2 would be interesting, but goes beyond the scope of the present

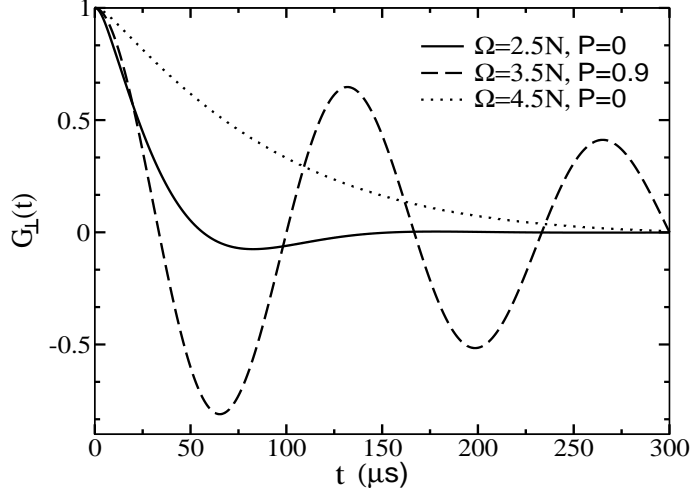


FIG. 8: The real part of the Green's function G_{\perp} for different regime of T_2 . G_{\perp} is evaluated by performing the inverse Fourier transform with Eq. (14). We have only plotted the envelope function of the correlation function. The actual evolution should be modulated by a fast oscillation with frequency Ω .

paper.

Obviously the T_2 time is proportional to the unit N/A . Therefore a larger quantum dot [with a larger number of nuclear spins (N)] has a longer T_2 time. In the bulk limit the coherence time becomes infinitely large because the hyperfine coupling is homogeneous so that there is no fluctuation of nuclear field. In the other limit of a smaller quantum dot the profile of the electron wavefunction becomes sharper because of the strong confinement. One thus also anticipate increased T_2 time since the effective nuclear flip-flop is more difficult to realize energetically just like in the case of the dipolar coupling.²² These arguments indicate that there should be a certain point regarding the QD size where the decoherence effect is the most serious. However, in our present calculations we would not be able to reach the latter limit because we cannot discuss the influence of the distance among nuclear spins on the electron-mediated interaction when converting the sum over nuclear sites into integrals.

The real time dynamics of the transverse electron spin Green's function $G_{\perp}(t)$ can be obtained by performing the inverse Fourier transform using Eq. (14). In Fig. 8 we show the evolution of the envelope of $G_{\perp}(t)$ (the maximum values during each cycle) for various P and Ω combinations. The actual evolution of $G_{\perp}(t)$ oscillates coherently with frequency close to Ω . In the relative small-magnetic-field ($\leq 10T$) and low-polarization limit, the amplitude

of $G_{\perp}(t)$ decays rapidly and completely. On the other hand, the coherence of the electron spin can be maintained for a much longer period if $P = 0.9$ even without a very large Ω . We should mention that the 90% nuclear polarization could be realizable in future experiments using dynamical nuclear polarization by polarized electronic transport^{30,31} or circularly polarized photons^{29,32,33} through hyperfine interaction. The current experimental realizable nuclear polarization in QDs remains less than 50%.²⁹ Our approximation should still be accurate with such a large nuclear polarization, because the numbers of up and down nuclear spins are still in the same order of magnitude at $P = 0.9$. If we go to the extremely polarized limit, the decoherence effect should become negligible as in the case of fully polarized nuclei. For the curve with $P = 0.9$, we also observe that there is a clear revival for $G_{\perp}(t)$ even after 100 microseconds.

With our approach we can identify the long time asymptotic behavior of $G_{\perp}(t)$. Again, the contour shown in Fig. 4 can be used to calculate the asymptotic integrals of Eq. (14) as $t \rightarrow \infty$ with the method of steepest descent. For simplicity we will only consider the effect of $\Sigma_1(\tilde{\omega})$. To evaluate these integrals we need to find the asymptotic form of the spectral function. The calculation is similar to what we have done for the low frequency solution. On the contours of C_2 and C_3 in Fig. 4, we define $\tilde{\omega} = 0^{\mp} - is$. On the contours of C_1 and C_4 , we replace $\tilde{\omega}$ by $\mp\frac{1}{2} - is$. Here s is a new real variable. The long time ($t \rightarrow \infty$) behavior is determined by the asymptotic form of the spectral function as $s \rightarrow 0^+$. On C_2 and C_3 , we find

$$\rho(0^{\mp} - is) = \frac{24\Omega^2}{\pi^2(1 - P^2)N^2}(1 \mp 3is) + O(s^3). \quad (58)$$

Performing the integral along the contours C_2 and C_3 as $t \rightarrow \infty$, we find

$$G_{\perp}(t) \propto \frac{144\Omega^2}{\pi^2(1 - P^2)N^2} \frac{1}{t^2}. \quad (59)$$

On the contours C_1 and C_4 , $\rho(\mp\frac{1}{2} - is) \propto s^2$. Therefore, the integral along C_1 and C_4 has a contribution of $\frac{1}{t^3}$ which is negligible compared to $\frac{1}{t^2}$ at long time limit. This non-exponential long time decay behavior is slower than that of the low-energy solution with strong magnetic field, where the form of $\frac{1}{t}$ is found. The $\frac{1}{t^2}$ behavior here is obtained by only considering $\Sigma_1(\tilde{\omega})$. The inclusion of $\Sigma_2(\tilde{\omega})$ is too complicated. However, we would expect power-law decay instead of the $\frac{1}{\text{int}}$ decay which appears in the solution for the low-energy solution in the absence of external magnetic field. Notice that the expression in Eq. (59)

diverges as the nuclear polarization goes toward 1. However, this is insignificant since our discussions in this subsection apply to partially and unpolarized nuclei so that P is always less than 1. Instead, the low energy solution has the right limit when $P = 1$. This is because both the exact solution of fully polarized nuclei and the low energy solution include only the real electron-nuclei flip-flop, while the high energy solution found in this section is due completely to the higher-order processes, which are only significant when $P < 1$.

IV. DISCUSSION

The calculations given in this paper can be generalized in several ways. Firstly, although we have been dealing with nuclei of spin $\frac{1}{2}$ exclusively throughout this paper, our study can be easily extended to nuclei with higher spin values. The qualitative behavior of the spectral function and the long time decay we have discovered here should not be modified in any significant way by considering nuclei with larger spins. Secondly, we have assumed a relatively simple form of the hyperfine coupling constant as a function of the position of the nucleus at \mathbf{r}_k , i.e., $A_k = e^{-\frac{k}{N}}$, to simplify the algebra. This form of A_k corresponds to a two-dimensional quantum dot with Gaussian electron wavefunction. However, our derivations and approximations are not limited by this choice of A_k and are applicable to any form of quantum dot with arbitrary electronic wavefunction. In short, all our results before converting the summations into integrals are correct for a general electron wavefunction. Generalization to a 3-dimensional quantum dot is more complicated mathematically because one would encounter integrations that cannot be performed analytically when converting the sums over nuclear lattice sites to integrals.

A more challenging and interesting generalization of the present work is to consider smaller effective magnetic fields, for example with $\Omega \sim O(\sqrt{N})$. It is well-known that the thermal statistical fluctuating nuclear magnetic field has this order of magnitude.³⁴ In such a case, our large N expansion can still be applied, because \sqrt{N} is still much larger than A_k . The Zeeman energy mismatch determines that the direct electron-nuclei relaxation effect is still negligible. However, the large field expansion we have developed in this paper loses its power in this situation since the expansion parameter $\frac{N}{\Omega} \gg 1$. Basically one has to consider more higher-order correlation functions with more pairs of flip-flopping nuclear spins. We expect this to be a very difficult task for analytical calculations.

We have studied the Non-Markovian dynamics of electron spin with the nuclear spin reservoir in an initial product state. It has recently been found that the electron spin dynamics shows different behaviors for randomly correlated initial nuclear spin states or ensemble averaged initial states.¹⁰ Our analytical results can be directly used to investigate the electron spin decoherence by summing over the product states in the ensemble. Our treatment can also be applied to study the Non-Markovian spin dynamics of spin-boson model, where a single spin interacts with a reservoir of bosons at thermal equilibrium in the initial state. It would also be interesting to extend the approach presented in this paper to study the dephasing time of two-electron spin states in double QD, where both the T_2^* and T_2 has been measured.²

V. CONCLUSIONS

To summarize, we have obtained the *decoherence* of a single electron spin confined in a quantum dot with large effective magnetic fields (including both external field and nuclear field) by computing the Green's function $G_{\perp}(t)$ for the electron spin using the equation-of-motion method. We have solved this problem for three types of initial nuclear spin states, the fully polarized case, the almost fully polarized case with one nuclear spin flipped, and the more general partially polarized and unpolarized cases. We have found that the spectral functions have quite different properties at the low frequency ($\omega \sim A/N$) and the high frequency region ($\omega \sim A$). By comparing the exact solution of fully polarized nuclei and the solution of almost fully polarized cases, we demonstrate that the virtual nuclear spin flip-flop leads to a new feature in the high energy limit. Our studies of electron spin decoherence in the low energy region recover previous results, which did not include these higher-order processes. Namely, the decay amplitude is of the order $O\left(\frac{1}{N}\right)$. More importantly, we have also obtained the solution of partially polarized and unpolarized nuclei by considering the indirect nuclear spin flip-flop explicitly, helped with a large field expansion method. We find that the electron spin T_2 time is very sensitive to nuclear polarization when $P > 0.6$, and the electron spin coherence time can be enhanced by 10 times if the nuclear polarization is increased to 90%. We also find that this decoherence is complete, and the long time asymptotic behavior of the Green's function representing the transverse electron spin dynamics is $\frac{1}{t^2}$.

Acknowledgments

We acknowledge financial support by NSA, LPS, and ARO.

APPENDIX A: EXACT SOLUTION OF FULLY POLARIZED NUCLEI IN JORDAN-WIGNER REPRESENTATION

For spin one-half nuclei, we can introduce the Jordan-Wigner representation:³⁵

$$\begin{aligned} S^+ &= d, \quad S^- = d^\dagger, \quad S^z = \frac{1}{2} - n_d \\ I_k^+ &= e^{-i\pi n_d} a_k, \quad I_k^- = a_k^\dagger e^{i\pi n_d}, \quad I_k^z = \frac{1}{2} - n_k, \end{aligned} \quad (\text{A1})$$

where $n_d = d^\dagger d$ and $n_k = a_k^\dagger a_k$. All operators obey the standard fermion anti-commutation relations: $\{d, d^\dagger\} = 1$; $\{a_k, a_k^\dagger\} = 1$. This representation preserves all spin commutation relations except for those of two nuclear spin operators at two different lattice sites. However these commutators are not necessary for fully polarized nuclei, because there should be only one flipped spin at any moment during the evolution. In terms of correlation functions, this means we won't encounter any correlation function containing two nuclear operators so that there is no problem of ordering different nuclear spin operators using the fermion operators.

Transforming the original Hamiltonian of Eq. (1) into the new representation, we arrive at

$$\begin{aligned} H_{\text{JW}} &= - \sum_k \frac{A_k}{2} n_k - \left(\omega_0 + \frac{A}{2} \right) n_d \\ &+ \sum_k \frac{A_k}{2} (a_k^\dagger d + d^\dagger a_k), \end{aligned} \quad (\text{A2})$$

where $A = \sum_k A_k$. We have ignored a constant term in the derivation. The quartic interaction term $\sum_k A_k n_k n_d$ in H_{JW} is dropped because $\sum_k A_k n_k$ and n_d cannot both be 1 (down state). The new Hamiltonian H_{JW} is in the form of the non-interacting Anderson impurity model,²⁶ describing a localized state (electron spins) interacting with semi-continuous states represented by the nuclear spins. This is the key feature that we focus in this paper: a single electronic spin interacts with many nuclear spins with different strengths. The non-interacting Anderson impurity model can be solved exactly. Specifically, the exact solution

of H_{JW} for the Green's function $\langle\langle d; d^+ \rangle\rangle_\omega$ is²⁵

$$\langle\langle d; d^+ \rangle\rangle_\omega = \frac{1}{\omega + \omega_0 + \frac{A}{2} - \frac{1}{4} \sum_k \frac{A_k^2}{\omega + \frac{A_k}{2}}}. \quad (\text{A3})$$

The spectral function $(-\text{Im}\langle\langle d; d^+ \rangle\rangle_\omega/\pi)$ that represents the overlapping of the localized state with the exact eigenstate is the same as what we have found in Section III.

APPENDIX B: EOMS FOR THE POLARIZED NUCLEAR RESERVOIR WITH ONE-FLIPPED NUCLEAR SPIN

The EOMs are generated by computing the commutators in Eq. (9). The highest order correlation functions that survive are those which involve two spin-lowering operators, either S^- or I_k^- . All higher order functions with more spins flipped to down direction vanish because the total angular $(\sum_k A_k I_k^z + S^z)$ momentum along z direction (of the external field) is a constant of motion. Explicitly, the equations are:

$$\left[\omega - \Omega - \Sigma_0(\omega) + A_k + \frac{A_k^3}{4(\omega^2 - A_k^2/4)} \right] \langle\langle n_k S^-; S^+ \rangle\rangle_\omega = \langle \Psi_0 | n_k | \Psi_0 \rangle - \frac{1}{4} \sum_{k'(k)} \frac{A_k A_{k'} V_{kk'}(\omega)}{\omega + A_k/2} - \frac{1}{4} \sum_{k'(k)} \frac{A_k A_{k'} V_{k'k}(\omega)}{\omega - A_{k'}/2}, \quad (\text{B1})$$

$$\left(\omega - \frac{A_{k'}}{2} \right) \langle\langle n_k I_{k'}^-; S^+ \rangle\rangle_\omega = -\frac{A_{k'}}{2} \langle\langle n_k S^-; S^+ \rangle\rangle_\omega + \frac{A_k}{2} V_{kk'}(\omega), \quad (\text{B2})$$

$$\begin{aligned} \left(\omega + \Omega - \frac{A_k + A_{k'}}{2} \right) \langle\langle I_k^- S^+ I_{k'}^-; S^+ \rangle\rangle_\omega &= \frac{A_k}{2} \langle\langle n_k I_{k'}^-; S^+ \rangle\rangle_\omega + \frac{A_{k'}}{2} \langle\langle I_k^- n_{k'}; S^+ \rangle\rangle_\omega \\ &- \frac{A_k}{2} \langle\langle I_{k'}^- \left(\frac{1}{2} - S^z \right); S^+ \rangle\rangle_\omega - \frac{A_{k'}}{2} \langle\langle I_k^- \left(\frac{1}{2} - S^z \right); S^+ \rangle\rangle_\omega \\ &+ \sum_{k''(k, k')} \frac{A_{k''}}{2} \langle\langle I_k^- I_{k''}^+ I_{k'}^-; S^+ \rangle\rangle_\omega, \end{aligned} \quad (\text{B3})$$

$$\begin{aligned} \left(\omega - \Omega + \frac{A_k + A_{k'}}{2} \right) \langle\langle I_k^- I_{k'}^+ S^-; S^+ \rangle\rangle_\omega &= \frac{A_{k'}}{2} \langle\langle I_k^- \left(\frac{1}{2} - S^z \right); S^+ \rangle\rangle_\omega \\ &- \frac{A_{k'}}{2} \langle\langle I_k^- n_{k'}; S^+ \rangle\rangle_\omega - \sum_{k''(k, k')} \frac{A_{k''}}{2} \langle\langle I_k^- I_{k'}^+ I_{k''}^+; S^+ \rangle\rangle_\omega, \end{aligned} \quad (\text{B4})$$

$$\begin{aligned} \left(\omega - \frac{A_k + A_{k''} - A_{k'}}{2} \right) \langle\langle I_k^- I_{k'}^+ I_{k''}^-; S^+ \rangle\rangle_\omega &= -\frac{A_k}{2} \langle\langle I_{k''}^- I_{k'}^+ S^-; S^+ \rangle\rangle_\omega \\ &+ \frac{A_{k'}}{2} \langle\langle I_k^- S^+ I_{k'}^-; S^+ \rangle\rangle_\omega - \frac{A_{k''}}{2} \langle\langle I_k^- I_{k'}^+ S^-; S^+ \rangle\rangle_\omega. \end{aligned} \quad (\text{B5})$$

Together with Eqs. (10), these equations form a closed set. The full solution of these equations is mathematically intractable because of the number of equations involved. In

Section III, we find approximate solutions in the low frequency ($\omega \sim 1$) and high frequency ($\omega \sim \Omega$) regions using $\frac{1}{N}$ expansion.

APPENDIX C: EVALUATION OF $\sigma_n(\omega)$

In this appendix the real and imaginary parts of the terms $\sigma_n(\omega)$ [defined in Eq. (42)] appearing in the low energy solution of partially polarized and unpolarized nuclei in Section III are calculated. The spectral function of the electron spin correlation function calculated from $\sigma_n(\omega)$ can be used to obtain the renormalized spin precession frequency and decay of electron spin coherence. There are three steps in these calculations. First we perform analytical continuation by replacing ω with $\omega + i0^+$ to obtain the retarded expressions. We then use the relation $\frac{1}{x+i0^+} = P\frac{1}{x} - i\pi\delta(x)$ to separate the principle values and the imaginary parts. Finally we convert the summation over the nuclear sites into an integral, $\sum_k \rightarrow \int_0^\infty dk$. The validity and efficiency of this conversion have been discussed before.¹¹

Recall that the summation $\sigma_2(\omega)$ is

$$\sigma_2(\omega) = \sum_k \frac{A_k}{\omega - \frac{A_k}{2}} - \sum_k \frac{A_k}{\omega + \frac{A_k}{2}}. \quad (\text{C1})$$

Using the procedures described above we find that the real and imaginary parts of $\sigma_2(\omega)$ are

$$\text{Re } \sigma_2(\omega) = -2N \left[\ln \left| 1 + \frac{1}{2\omega} \right| + \ln \left| 1 - \frac{1}{2\omega} \right| \right], \quad (\text{C2})$$

and

$$\text{Im } \sigma_2(\omega) = \begin{cases} -2N\pi & 0 < \omega < \frac{1}{2} \\ 2N\pi & -\frac{1}{2} < \omega < 0. \end{cases} \quad (\text{C3})$$

$\sigma_3(\omega)$ and $\sigma_4(\omega)$ can be evaluated in a similar manner. We obtain

$$\text{Re } \sigma_3(\omega) = -4N + 4N\omega \ln \left| \frac{2\omega + 1}{2\omega - 1} \right|, \quad (\text{C4})$$

$$\text{Im } \sigma_3(\omega) = -4N\pi\omega, \quad -\frac{1}{2} < \omega < \frac{1}{2}, \quad (\text{C5})$$

$$\text{Re } \sigma_4(\omega) = -2N - 8N\omega^2 \left[\ln \left| 1 + \frac{1}{2\omega} \right| + \ln \left| 1 - \frac{1}{2\omega} \right| \right], \quad (\text{C6})$$

and

$$\text{Im } \sigma_4(\omega) = \begin{cases} -8N\pi\omega^2 & 0 < \omega < \frac{1}{2} \\ 8N\pi\omega^2 & -\frac{1}{2} < \omega < 0, \end{cases} \quad (\text{C7})$$

Both $\omega = \pm\frac{1}{2}$ and $\omega = 0$ are branch points for the self-energy. The two branch cuts ($[-1/2, 0]$ and $[0, 1/2]$) come from different dynamical fields of the electron felt by the nucleus, i.e., $\frac{A_k}{4}$ when $S^z = \frac{1}{2}$, and $-\frac{A_k}{4}$ when $S^z = -\frac{1}{2}$. In contrast only $\omega = -\frac{1}{2}$ appears as a branch point in the fully polarized case because $S^z = 1/2$ ($n_d = 0$) makes no contribution to the Hamiltonian in A2.

APPENDIX D: EVALUATION OF SELF-ENERGY TERMS, $\Sigma_1(\tilde{\omega})$, $\Sigma_2(\tilde{\omega})$, AND $\Sigma_3(\tilde{\omega})$

Using the definitions of the self-energy terms given in Eqs. (55), (56) and (57), and converting the summations into integrals, we can obtain analytical expressions of the real and imaginary parts of these self-energy terms. The same procedures as we have described in Section C are used in the following calculations. We find

$$\Sigma_1(\tilde{\omega}) = \sum_{k,k'} \frac{A_k^2 A_{k'}^2}{\tilde{\omega} + \frac{A_k - A_{k'}}{2}} = N^2 \int_0^1 dx \int_0^1 dy \frac{xy}{\tilde{\omega} + \frac{x-y}{2}}, \quad (\text{D1})$$

where we have written A_k and $A_{k'}$ as the integral variables x and y . The two-dimensional integral can be calculated, so that

$$\begin{aligned} \text{Re } \Sigma_1(\tilde{\omega}) &= -\frac{2N^2}{3} \left[\tilde{\omega} + 4\tilde{\omega}^3 \ln \left| 1 - \frac{1}{4\tilde{\omega}^2} \right| \right. \\ &\quad \left. - 3\tilde{\omega} \ln \left| 1 - \frac{1}{4\tilde{\omega}^2} \right| + \ln \left| \frac{2\tilde{\omega} - 1}{2\tilde{\omega} + 1} \right| \right], \end{aligned} \quad (\text{D2})$$

and

$$\text{Im } \Sigma_1(\tilde{\omega}) = -\frac{2N^2}{3} [4|\tilde{\omega}|^3 - 3|\tilde{\omega}| + 1]. \quad (\text{D3})$$

Again, the imaginary part of $\Sigma_1(\tilde{\omega})$ is nonvanishing only when $-\frac{1}{2} < \tilde{\omega} < \frac{1}{2}$. Similarly,

$$\Sigma_2(\tilde{\omega}) = N^3 \int_0^1 dx \int_0^1 dy \int_0^1 dz \frac{xyz}{(\tilde{\omega} + \frac{x-y}{2})(\tilde{\omega} + \frac{x-z}{2})}. \quad (\text{D4})$$

$$\text{Re } \Sigma_2(\tilde{\omega}) = 4N^3 \int_0^1 ds \, s \left[1 + (2\tilde{\omega} + s) \ln \left| \frac{2\tilde{\omega} + s - 1}{2\tilde{\omega} + s} \right| \right] \quad (\text{D5})$$

$$\text{Im } \Sigma_2(\tilde{\omega}) = \begin{cases} \frac{1}{2} - \ln|1 - 2\tilde{\omega}| - 2\tilde{\omega} + \frac{8\tilde{\omega}}{3}\ln|1 - 2\tilde{\omega}| + \frac{10\tilde{\omega}^2}{3} \\ - \frac{8\tilde{\omega}^3}{3} - \frac{16\tilde{\omega}^4}{3}\ln\left|\frac{1}{2\tilde{\omega}} - 1\right|, & 0 < \tilde{\omega} < \frac{1}{2} \\ \frac{1}{2} - 2\tilde{\omega} - 8\tilde{\omega}\ln|1 - 2\tilde{\omega}| + \frac{16\tilde{\omega}^2}{3}\ln|1 + 2\tilde{\omega}| \\ + 8\tilde{\omega}^2\ln\left|\frac{1}{2\tilde{\omega}} + 1\right| - \frac{14\tilde{\omega}^2}{3} + \frac{8\tilde{\omega}^3}{3} \\ - \frac{16\tilde{\omega}^4}{3}\ln\left|\frac{1}{2\tilde{\omega}} + 1\right|, & -\frac{1}{2} < \tilde{\omega} < 0, \end{cases}$$

Repeating the calculation for $\Sigma_3(\tilde{\omega})$, we find that $\Sigma_3(\tilde{\omega}) = \Sigma_2(\tilde{\omega})$. The integral in Eq. (D5) can be computed numerically. However, the calculation is non-trivial because of the singularities appearing in the expression. Alternatively, the integral can be done analytically using Maple. The result, which is too complicated to be presented here, is a sum of terms that include the dilog functions defined as $f_{\text{dilog}}(x) = \int_0^x \ln t/(1-t)dt$.³⁶ Numerical calculation of the real part of $\Sigma_2(\tilde{\omega})$ using the analytical expression obtained with Maple is very accurate when we check the sum rule of the spectrum function numerically (see discussion in Section III).

-
- ¹ T. Fujisawa, D.G. Austing, Y. Tokura, Y. Hirayama, and S. Tarucha, *Nature* **419**, 278 (2002).
- ² J.R. Petta, A.C. Johnson, J.M. Taylor, E.A. Laird, A. Yacoby, M.D. Lukin, C.M. Marcus, M.P. Hanson, and A.C. Gossard, *Science* **309**, 2180 (2005).
- ³ F.H.L. Koppens, J.A. Folk, J.M. Elzerman, R. Hanson, L.H. Willems van Beveren, I.T. Vink, H.P. Tranitz, W. Wegscheider, L.P. Kouwenhoven, and L.M.K. Vandersypen, *Science* **309**, 1346 (2005).
- ⁴ F. H. L. Koppens, C. Buizert, K. J. Tielrooij, I. T. Vink, K. C. Nowack, T. Meunier, L. P. Kouwenhoven, L. M. K. Vandersypen, *Nature* **442**, 766 (2006).
- ⁵ X. Hu and S. Das Sarma, *Phys. Status Solidi B* **238**, 360 (2003); X. Hu, in *Quantum Coherence*, edited by W. Potz, J. Fabian, and U. Hohenester, Lecture Notes in Physics Vol. 689 (Springer, Berlin, 2006), pp. 83-114; S. Das Sarma, R. de Souda, X. Hu, and B. Koiller, *Solid State Commun.* **133**, 737 (2004).
- ⁶ D. Loss, and D.P. DiVincenzo, *Phys. Rev. A* **57**, 120 (1998).
- ⁷ J.M. Taylor *et al*, *Nature Physics* **1**, 177 (2005).

- ⁸ J.M. Taylor, C.M. Marcus, and M.D. Lukin, Phys. Rev. Lett. **90**, 206803 (2003); J.M. Taylor, A. Imamoglu, and M.D. Lukin, Phys. Rev. Lett. **91**, 246802 (2003).
- ⁹ A. Khaetskii, D. Loss, and L. Glazman, Phys. Rev. Lett. **88**, 186802 (2003); A. Khaetskii, D. Loss, and L. Glazman, Phys. Rev. B **67**, 195329 (2003).
- ¹⁰ J. Schliemann, A.V. Khaetskii, and D. Loss, Phys. Rev. B **66**, 245303 (2002).
- ¹¹ W.A. Coish and D. Loss, Phys. Rev. B **70**, 195340 (2004).
- ¹² S.I. Erlingsson and Y.V. Nazarov, Phys. Rev. B **70**, 205327 (2004).
- ¹³ N. Shenvi, R. de Sousa, and K.B. Whaley, Phys. Rev. B **71**, 224411 (2005).
- ¹⁴ W. Yao, R.B. Liu, and L.J. Sham, cond-mat/0508441 (2005); cond-mat/0604634 (2006).
- ¹⁵ C. Deng and X Hu, Phys. Rev. B **73**, 241303(R) (2006).
- ¹⁶ K.A. Al-Hassanieh, V.V. Dobrovitski, E. Dagotto, and B.N. Harmon, Phys. Rev. Lett. **97**, 037204 (2006)
- ¹⁷ U. Weiss, *Quantum Dissipative Systems* (World Scientific, Singapore, 2001).
- ¹⁸ I.A. Merkulov, A.L. Efros, and M. Rosen, Phys. Rev. B **65**, 205309 (2002).
- ¹⁹ C.P. Slichter, *Principles of Magnetic Resonance* (Springer-Verlag, Berlin, 1996).
- ²⁰ N. Bloembergen and T.J. Rowland, Phys. Rev. **97**, 1679 (1955).
- ²¹ V.N. Golovach, A. Khaetskii, and D. Loss, Phys. Rev. Lett. **93**, 016601 (2004).
- ²² R. de Sousa and S. Das Sarma, Phys. Rev. B **67**, 033301 (2003); *ibid.* **68**, 115322 (2003).
- ²³ W.M. Witzel and S. Das Sarma, Phys. Rev. B **72**, 161306(R) (2005).
- ²⁴ A. Abragam, *The Principles of Nuclear Magnetism* (Oxford University Press, London, 1961).
- ²⁵ G.D. Mahan, *Many-Particle Physics*, (Plenum Press, New York, 1990).
- ²⁶ P.W. Anderson, Phys. Rev. **124**, 41 (1961).
- ²⁷ C.M. Bender and S.A. Orszag, *Advanced Mathematical Methods for Scientists Engineers*, (Springer, 1999).
- ²⁸ D. Paget, G. Lampel, B. Sapoval, and V.I. Safarov, Phys. Rev. B, **15**, 5780 (1977).
- ²⁹ D. Gammon, E.S. Snow, B.V. Shanabrook, D.S. Katzer, and D. Park, Phys. Rev. Lett. **76**, 3005 (1996).
- ³⁰ K. Ono and S. Tarucha, Phys. Rev. Lett. **92**, 256803 (2004).
- ³¹ C. Deng and X Hu, Phys. Rev. B **71**, 033307 (2005).
- ³² A. Imamoglu, E. Knill, L. Tian, and P. Zoller, Phys. Rev. Lett. **91**, 017402 (2003).
- ³³ C. W. Lai, P. Maletinsky, A. Badolato, and A. Imamoglu, Phys. Rev. Lett. **96**, 167403 (2006).

³⁴ F. Meier and B.P. Zakharchenya, *Optical Orientation*, (North Holland, Amsterdam, 1984).

³⁵ T. Giamarchi, *Quantum Physics in One Dimension*, (Clarendon Press, Oxford, 2004).

³⁶ M. Abramowitz and I.A. Stegun, *Handbook of Mathematical Functions With Forms, Graphs, and Mathematical Tables*, (National Bureau of Standards, 1964).